sciendo
Austrian Journal of Earth Sciences | Vienna | 2025 | Volume 118 | 41–60 | DOI: 10.17738/ajes.2025.0002

# Petrography, sedimentology and Neoalpine metamorphism of the Idalp ophiolite, Steinsberg and Idalp formations, Lower Engadine Window, Tyrol (Austria)

Peter Tropper[1*], Karl Krainer[2], Ansgar Frese[1], Gabriel Raso[2]

[1)] Institute of Mineralogy and Petrography, University of Innsbruck, Innrain 52f, 6020 Innsbruck, Austria
[2)] Institute of Geology, University of Innsbruck, Innrain 52f, 6020 Innsbruck, Austria
[*)] Corresponding author: Peter Tropper

**Keywords:** Lower Engadine Window, ophiolite, carbonate sediments, siliciclastic sediments, Neoalpine metamorphism, geothermobarometry, Tyrol

## Abstract

The Lower Engadine Window is the only tectonic window in the Eastern Alps in which all three Penninic nappes are exposed. The focus of this study lies on the sedimentologic investigation of the Jurassic Steinsberg and Idalp formations of the Middle Penninic Nappe system, the petrographic investigation of the Idalp ophiolite of the Upper Penninic Nappe system, and on the study of the Neogene metamorphism of these rocks. The Steinsberg Formation, composed of carbonate sediments rich in crinoid fragments ("encrinites"), accumulated in a shallow, normal marine depositional setting on the shelf of the Iberia-Briançonnais microcontinent. Overlying sediments of the Idalp Formation, represented by shale and intercalated sandstone, are interpreted to be of a deeper marine shelf setting. Rocks of the Idalp ophiolite represent fragments of the oceanic crust of the Piemont-Liguria Ocean. The obtained multi–equilibrium *P-T* estimates using the program THERMOCALC v.3.33 from two metagabbro samples (amphibole + chlorite + pumpellyite + albite + quartz ± muscovite ± clinopyroxene) yield pressures of 0.63 to 0.95 GPa and temperatures between 330 °C and 390 °C (Mode-1 invariant points), 0.70 to 0.80 GPa and temperatures between 340 °C and 360 °C (Mode-2 with and without clinopyroxene). These data are in good agreement with the data of Höck et al. (2004) which are 0.7–0.9 GPa at approx. 350 °C. For the first time *T*-data of 330 ± 25 °C were obtained from a calcareous sandstone of the Idalp Formation of the Middle Penninic Nappe system using calcite-dolomite geothermometry. The *P-T* results indicate that the Idalp ophiolite underwent the Neoalpine regional metamorphism at low-*T*/high-*P* at the transition from upper greenschist- to blueschist-facies and that the Idalp Formation was also characterized by this low-*T* metamorphism. This metamorphic overprint was then followed by uplift on the European shelf and the uplift and later exhumation of the rocks of the Idalp ophiolite, and sedimentary rocks of the Steinsberg- and Idalp formations.

## 1. Introduction

In the Lower Engadine Window rocks of the Penninic Unit are exposed which originally were formed in the Piemont-Liguria Ocean, the Iberian-Briançonnais microcontinent and the Valais Ocean (Fig. 1a). The Penninic rocks of the Lower Engadine Window are overlain by Austrolpine nappes of the Silvretta Complex (assigned to the Silvretta-Seckau Nappe System sensu Schmid et al., 2004) in the north, the Ötztal Complex (assigned to the Ötztal-Bundschuh Nappe System sensu Schmid et al., 2004) in the southeast and east, and the Engadine Dolomites. The Penninic rocks of the Lower Engadine Window display a complex tectonic structure related to Neoalpine deformation and can be divided into three nappe systems (Schmid et al., 2004; Gruber et al., 2010; see also Tollmann, 1977; Oberhauser, 1980): (1) The Lower Penninic Nappes, which consist of rocks of the former Valais Ocean (Cretaceous - Paleogene). (2) The Middle Penninic

Nappes, which represent rocks of the Iberia-Briançonnais Microcontinent (Late Paleozoic to Paleogene), and (3) the Upper Penninic Nappes, which are composed of rocks of the former Piemont-Liguria Ocean (Jurassic - Cretaceous).

Data on the *P-T* conditions of the Neoalpine event of the Idalp ophiolite are now more than 30 years old and need to be re-examined by new geothermobarometric methods with robust statistical treatment of the data. No data exist on the metamorphism of the sediments of the Fimber Zone (Middle Penninic Nappes) including the Steinsberg- and Idalp Formations.

We studied sedimentary rocks of Jurassic age from the Middle Penninic Nappes (Steinsberg and Idalp formations) and magmatic rocks of the Idalp ophiolite (metagabbro, pillow basalt and radiolarite) of the Upper Penninic Nappes. In particular we provide (i) a detailed petrographic description of the Idalp ophiolite of the Upper Penninic Nappes (Bürkelkopf nappe) and new geothermobarometric data for the Neoalpine metamorphic peak and, (ii) a detailed stratigraphic and sedimentological description including microfacies analysis of the Jurassic Steinsberg and Idalp formations of the Fimber Zone (Middle Penninic Nappes) and preliminary estimates of their metamorphic *P-T* conditions.

## 2. Geologic background

### 2.1. Lower Penninic Nappes

The Lower Penninic Nappes include the Zone of Pfunds and Zone of Roz–Champatsch–Pezid (Fig. 1a). The dominant rocks are different types of calcareous mica schists and Bündnerschiefer that are of Cretaceous to Paleogene age. Fragments of the oceanic crust and upper mantle (ophiolites) are intercalated locally.

### 2.2. Middle Penninic Nappes

The Middle Penninic Nappes include the Fimber-Zone and Zone of Prutz - Ramosch (Fig. 1a). The Zone of Prutz - Ramosch is composed of Paleozoic phyllites, Alpine Verrucano, quartzite (Ladiser Quarzit), and Triassic carbonate rocks in its lower part. The upper part is interpreted as a mélange-zone that includes the Fimber Zone (Oberhauser, 1980; Gruber et al., 2010). This mélange-zone is composed of a matrix of upper Cretaceous to Paleogene metasediments („Höhere Flyschschiefer") with olistoliths and/or tectonic slices of Alpine Verrucano, quartzite (Ladiser Quarzit), Triassic carbonate rocks, Jurassic Steinsberger Kalk, Neokomschiefer and Tristel-Formation. The Fimber Zone consists mainly of upper Cretaceous to Paleogene metasediments and abundant tectonic slices and olistoliths. The stratigraphic succession of the Fimber Zone includes granitic and metamorphic basement rocks, which show Variscan metamorphic ages (Hunziker et al., 1992) that are overlain by metamorphically overprinted Triassic dolomites and limestones including rocks of the Upper Triassic Keuper facies. The Keuper facies is overlain by the Steinsberger Kalk that contains fossils which indicate Liassic age. Above follow *Posidonia* shales and Idalp sandstone that are in turn overlain by limestone breccias and limestone of Upper Jurassic (Malmian) age. The Lower Cretaceous succession includes calcareous schists with intercalated microbreccias (Neocomian Flysch) and fine-grained limestone breccias (Tristel Schichten), overlain by sandstones and breccias of Albian age and Couches Rouges of the Late Cretaceous. The youngest rocks are shales, sandstone and breccias which are termed „Bunte Bündnerschiefer" and are dated as Late Cretaceous to Eocene (Bertle, 2002; Bousquet et al., 2004; Oberhauser, 1980). Locally small tectonic slices of ophiolites are tectonically intercalated in the Fimber Zone (Gruber et al., 2010). The Fimber Zone is interpreted to represent the continental margin of the Briançonnais microcontinent or the marginal part of the Piemont-Liguria Ocean (Oberhauser, 2007; Bertle, 2002).

#### *2.2.1. Steinsberg Formation*

The Steinsberg Formation (Steinsberg-Kalk according to the lithologic lexicon of Switzerland (www.strati.ch) was first mentioned by Théobald (1864) as Steinsberger Lias, named after the castle ruins Steinsberg near the village of Ardez in the lower Engadine Valley (Switzerland) (Gruner, 1981). A type section has never been defined. Other names are Steinsberger Kalk (Gürler and Schmutz, 1995; Gruber et al., 2010) or Lias in Steinsberger Fazies (Cadisch, 1932). Fuchs and Oberhauser (1990) mapped the Steinsberger Kalk at a scale of 1:50 000. Therefore, this lithostratigraphic unit is a mappable unit of formation-rank and we use the term Steinsberg Formation.

The Steinsberg Formation is dated as Lower Jurassic (Sinémurian-Toarcian) based on the occurrence of ammonites and belemnites. The Steinsberg Formation is part of the Tasna Nappe (Iberia-Briançonnais-microcontinent) of the Middle Penninic Nappe System in the Lower Engadine Window. At the locality Muot da l´Hom north of Ardez Triassic dolomites are overlain by coarse-grained breccia containing clasts of dolomite, grayish-green limestone (? Rhaetian), greenish granite, quarzite, sericitschist and sericitegneiss. At the locality Craista Bischöf this breccia is overlain by Steinsberger Lias (Gruner, 1981). At Muot da l´Hom and south of Ardez a strongly deformed succession of flysch-like, dark brownish to black, rarely greenish schists and intercalated thin sandstone beds with a thickness of 20–50 m rests on the Steinsberg Formation. This succession is like the Panier Formation of the Falknis Nappe and to Middle Jurassic (Doggerian) sandstones of the Gelbhorn Nappe, Arosa Zone and Zone of Samaden (Gruner, 1981).

The Steinsberg Formation is lithologically divided into two units (members): the lower „Brachiopodenkalk" (member), overlain by the „Crinoidenkalk" (member). At the type locality Steinsberg near Ardez a complete section through the Steinsberg Formation is not exposed and the succession is tectonically deformed (Fig. 2). The succession is approximately 40 m thick, the contact to

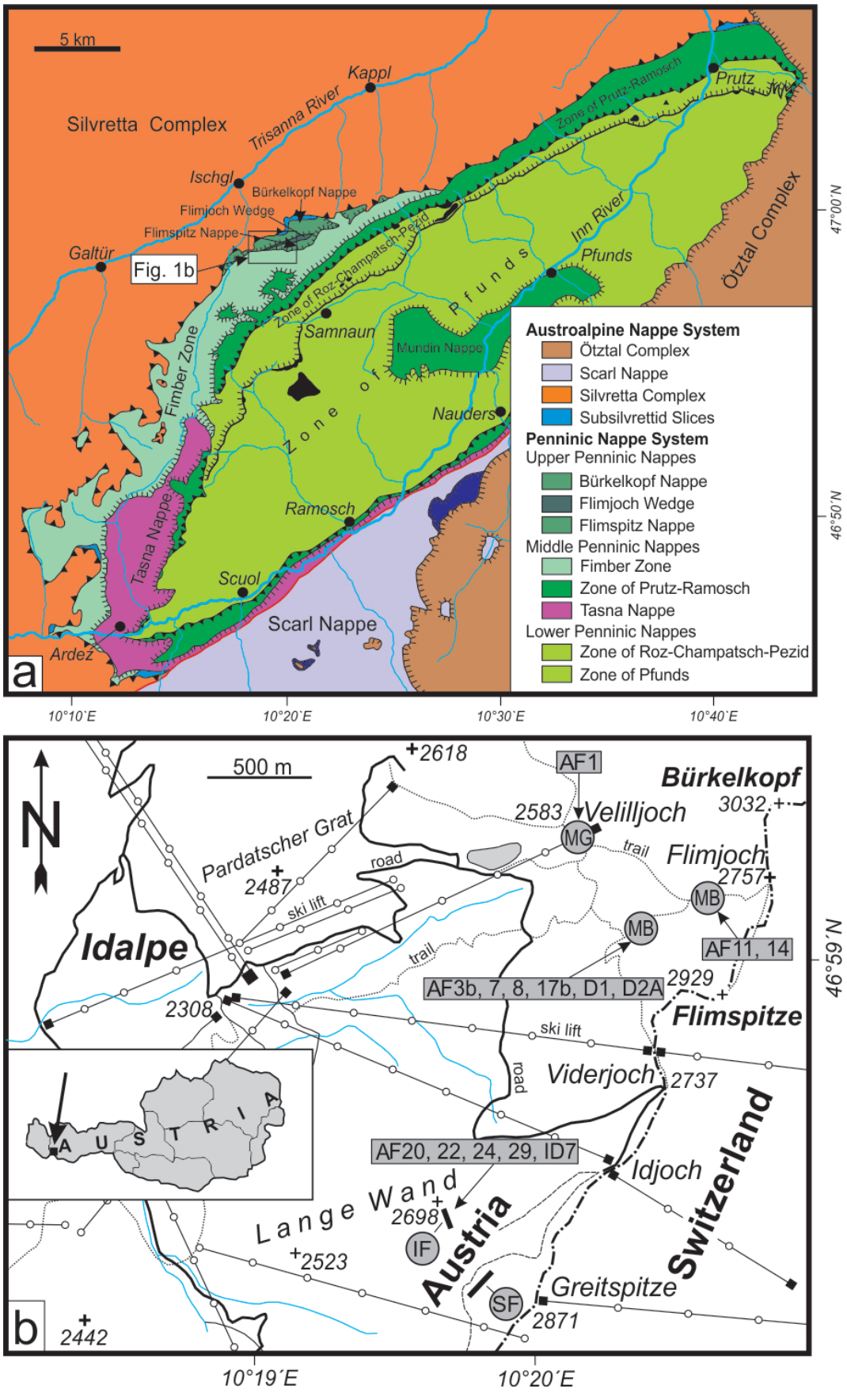


**Figure 1: (a)** Simplified geologic map of the Lower Engadine Window**, (b)** Map showing locations of the studied outcrops and samples. MG = metagabbro, MB = metabasalt, IF = stratigraphic section of the Idalp Formation, SF = stratigraphic section of the Steinsberg Formation.

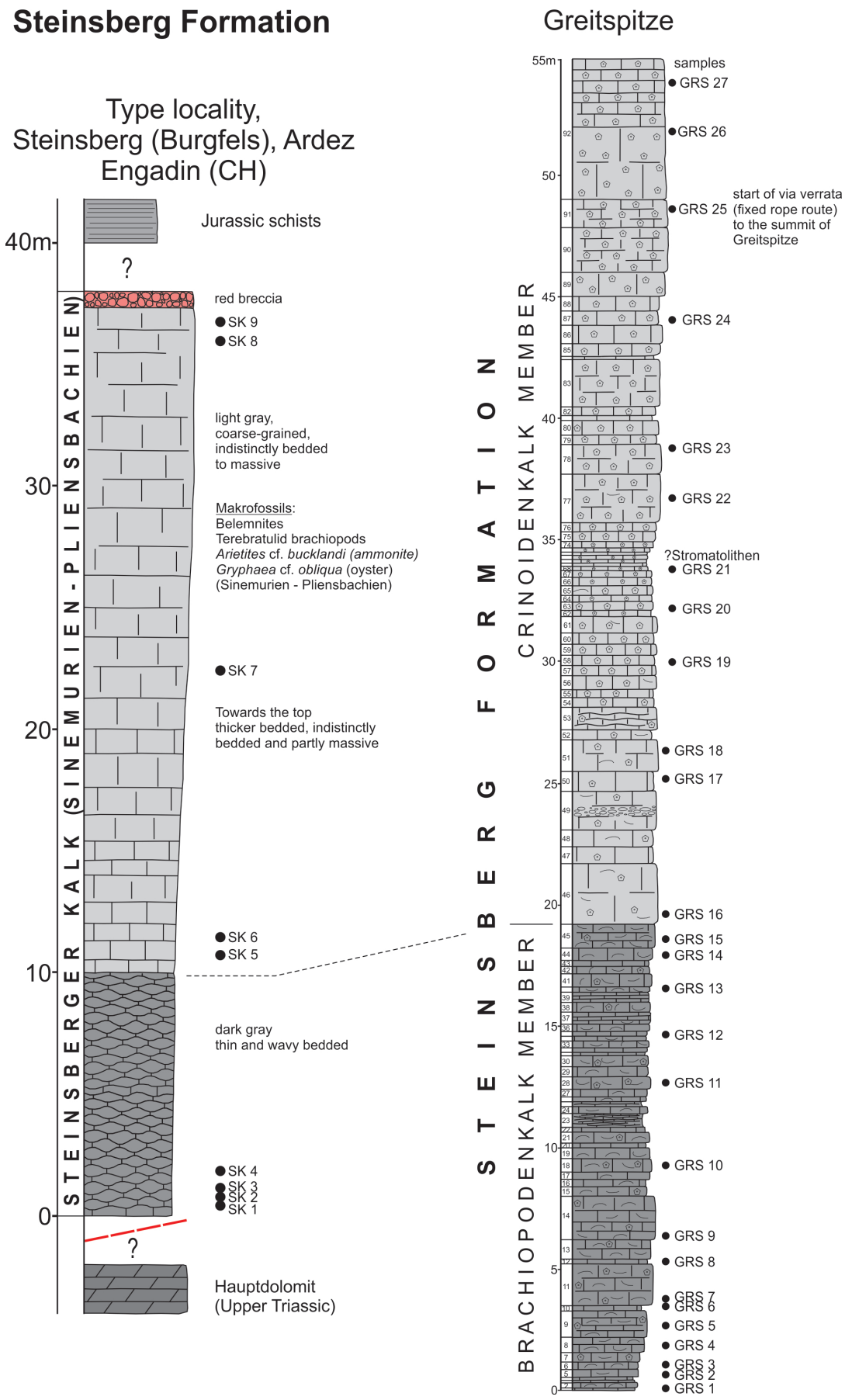


**Figure 2:** Stratigraphic section through the Steinsberg Formation at the type locality Steinsberg near Ardez and at the Greitspitze (location see Fig. 1b).

the underlying and overlying units is not exposed (see also Gürler and Schmutz 1995). The lower part (10 m) is thin- and wavy bedded, dark gray (Brachiopodenkalk-Member), grading upwards into thicker bedded to massive, light-gray limestone (Crinoidenkalk-Member). On top a thin red carbonate breccia containing fossils (crinoids) is developed. Gürler and Schmutz (1995) observed sandstone (2 m) and marl (1 m) at the base of the Steinsberger Kalk south of Steinsberg. The Steinsberg Formation is well exposed at the crest of Malfragenkopf approximately 4 km NNW of Spiss (Tyrol) where the succession rests on sandy marls with calcareous interbeds (Thum, 1966, 1970; Gruber et al., 2010). The overlying Steinsberg Formation starts with light gray limestone displaying graded bedding and containing poorly rounded quartz pebbles with diameters up to 2 cm. Above follow sandy to marly schists with calcareous interbeds and dark gray limestone containing ammonites, belemnites and crinoid fragments indicating Sinémurian age (Thum, 1966; Thum, 1970; Gruber, 2010). This basal succession is a few m thick and overlain by dark gray, partly sandy limestone with a thickness of approximately 20 m. These limestones contain brachiopods that indicate a middle lower Jurassic age and are termed „Brachiopodenkalk" (Gruber et al., 2010). The Brachiopodenkalk is overlain by light gray limestone composed mainly of crinoidal debris (Crinoidenkalk). Steinsberger Lias of Lange Wand yielded ammonites of the *obtusum*-Zone (upper Sinémurien) (Oberhauser, 1977). At Lange Wand the Steinsberg Formation is underlain by upper Triassic sedimentary rocks (Keuper) (Oberhauser, 1977).

#### *2.2.2. Idalp Formation*

In the area of Lange Wand, the Steinsberg Formation is overlain by dark gray schists that contain imprints of bivalves and are termed Posidonienschiefer (*Posidonia* shale) (Liassic), overlain by micaceous sandstones for which Oberhauser (1976) introduced the term Idalp–Sandstein (Figs. 4, 5). The Idalp-Sandstein and intercalated schists contain ammonites and belemnites indicating Middle Jurassic (Doggerian) age (Oberhauser, 1976, 1980). WNW of Höllenspitze, approximately 2.5 km SW of Lange Wand, the Idalp-Sandstein is 150–300 m thick, probably resulting from Neoalpine deformation. There, sandstone beds appear massive with indistinctly developed graded bedding and load casts at the base (Oberhauser 1984). Schists contain belemnites, *Zoophycos* and *Chondrites* (Oberhauser, 1984). A detailed description of the Posidonienschiefer and Idalp-Sandstein (including a type section) is still lacking. On the geological map, sheet 170 Galtür, Fuchs and Oberhauser (1990) mapped the Idalp-Sandstein and used the term „Idalpsandsteinfolge" (micaceous sandstone with shale interbeds, Doggerian) which therefore is of formation rank. We propose the term Idalp Formation for the clastic succession overlying the Steinsberg Formation in the Idalpe area, including the Posidonienschiefer and Idalp-Sandstein of Oberhauser (1976, 1980, 1984). The succession is well exposed near the eastern end of Lange Wand where it is approximately 28 m thick.

### 2.3. Upper Penninic Nappes

The Upper Penninic Nappes include the Bürkelkopf- and Flimspitz slices. These tectonic slices represent rocks of the Upper Jurassic-Lower Cretaceous oceanic crust and upper mantle (ophiolites) and overlying deep-sea sediments of the Piemont-Liguria Ocean. These ophiolites (Idalp ophiolite) are composed of ultrabasic rocks, metagabbros, metamorphic pillow basalts and overlying deep-sea sediments (Höck and Koller, 1987, 1989; Höck et al., 1986, 2004; Koller and Höck, 1987, 1990; Koller et al., 1996). All rocks of the Lower Engadine Window were metamorphically overprinted during the Neoalpine metamorphic event.

The Idalp ophiolite is part of the Upper Penninic Nappes (Fig. 1a). The ophiolite is exposed in two independent units called Flimspitze nappe (southern part) and Bürkelkopf nappe (northern part, Daurer, 1980). These two ophiolite nappes are separated by a tectonic slice composed of retrogressed micaschists, gneisses, and amphibolites termed "Flimjoch wedge", which originated from the neighboring Austroalpine Silvretta Metamorphic Complex (Fig. 1a). The ophiolite sequence starts with serpentinites, which contain small inclusions of rodingites that represent metasomatized metagabbros. The serpentinites are separated from the overlying metagabbros by a tectonic contact. The metagabbros were intruded by diabase dikes. The volcanic succession shows a tectonic base and starts with pillow lavas intercalated with several layers of massive diabase, and intercalations of hyaloclastites that increase in abundance upsection. The top of the volcanic succession is composed of metatuffs that are overlain by radiolarian schists. The entire volcanic succession (including the sediments) is approximately 250 to 300 meters thick. The two tectonic subunits of the ophiolite complex consist of a serpentinite-gabbro succession with a maximum thickness of 150 meters at its base and on top a large recumbent fold overturned towards the north, consisting of a small serpentinite + metagabbro body in the core, surrounded by massive lava-flows and pillows. According to Höck et al. (2004) and Schuster et al. (2004) the metamorphic evolution of the ophiolites is twofold. An older high-*T* oceanic metamorphic event of possibly Jurassic age, can be separated from a younger Neoalpine HP overprint (42–40 Ma, Bertle et al., 2003; Wiederkehr et al., 2009). Evidence for the former metamorphic event comes from the replacement of gabbroic clinopyroxenes by amphiboles (pargasite, magnesian hornblende to actinolite), which formed at relatively high temperatures. This, together with some metasomatic changes of the bulk geochemistry (mainly Na enrichment), and some local strong oxidation, argues for this hydrothermal event. The cores of these amphiboles in the altered metagabbros

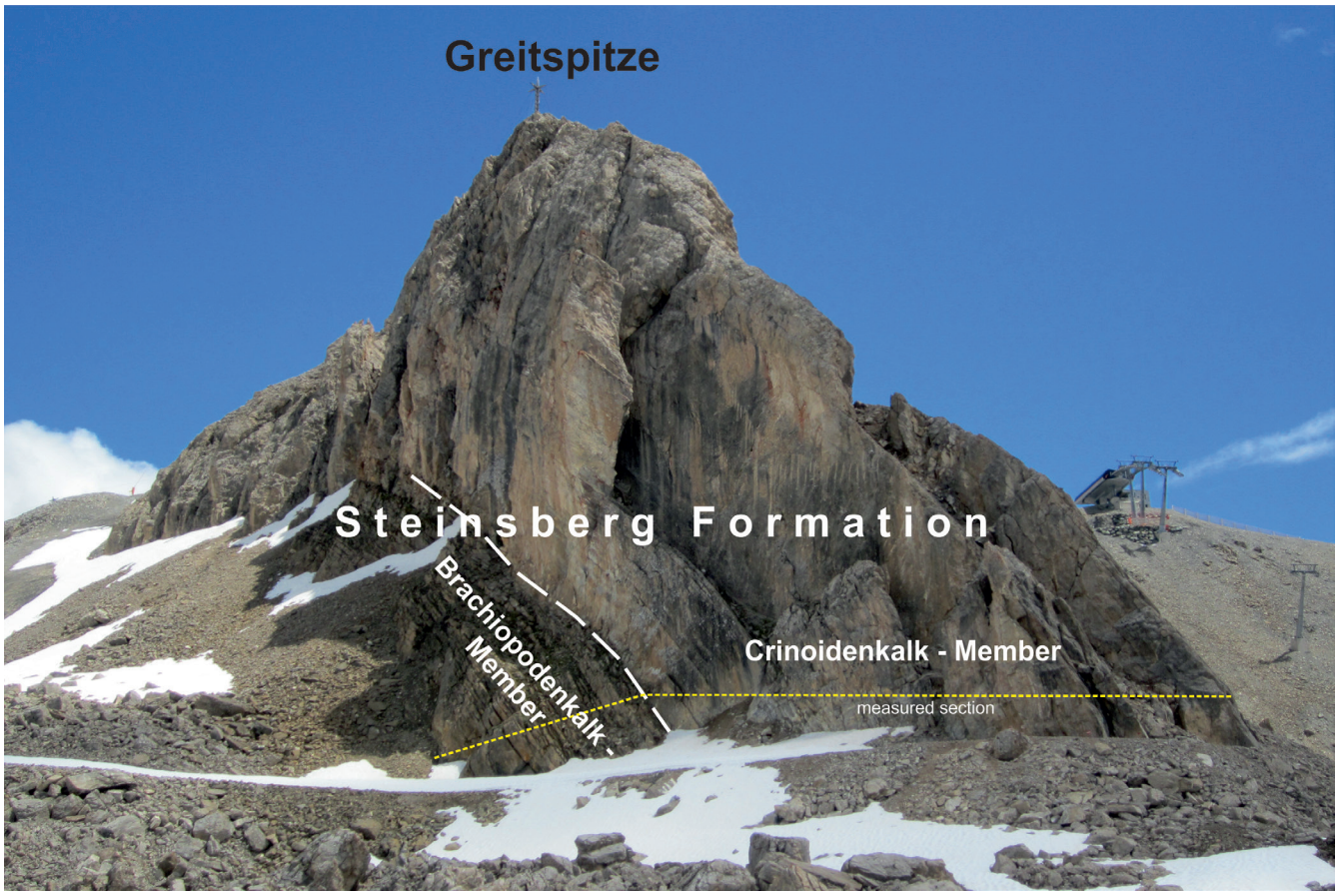


**Figure 3:** Greitspitze composed of Steinsberg Formation with darker, well bedded Brachiopodenkalk-Member and light gray, indistinctly thicker bedded Crinoidenkalk-Member. The stratigraphic section was measured along the yellow dashed line. View towards south.

still contain high Cl contents of up to 4000 ppm. In the hyaloclastites and pillow breccias, the hydrothermal influx locally causes ca. E-W striking epidote-rich veins, and high oxidation with an intense red color. The Neoalpine metamorphic grade of the Idalp ophiolite sequence is at the transition between greenschist and blueschist facies with *P-T* conditions of ca. 300–350 °C and 0.7–0.9 GPa (Koller, 1985; Höck et al., 2004). The mineral assemblages are defined by pumpellyite + chlorite + albite + epidote + actinolite + muscovite + titanite + hematite. Pumpellyite of the metagabbro is Mg–rich and pumpellyite compositions therefore plot into the blueschist-facies field in the Al-Fe-Mg ternary diagram after Barriga and Fyfe (1983). Tropper and Krainer (2017) provided additional *P-T* data using pseudo section calculations undertaken in the system $Na_2O$-CaO-$K_2O$-FeO-MgO-$Al_2O_3$-$SiO_2$-$H_2O$-$TiO_2$ (NCKFMASHT) using the program Theriak-Domino (De Capitani and Petrakakis, 2010) with an updated version of the internally consistent data set of Holland and Powell (1998, data set tcdb55). The pseudosection using the metagabbro bulk rock composition I48 from Höck and Koller (1987) yield a maximal *P-T* stability limit for assemblages containing pumpellyite without lawsonite and albite of 0.65 GPa at ca. 300 °C, which correlates well with previous estimates. If albite + pumpellyite coexist the maximal pressure is 0.5 GPa at 300 °C. These calculations are only of semiquantitative nature since they also assume a rather complex mineral assemblage containing omphacite + muscovite + paragonite + pumpellyite + epidote + titanite ± albite, which has not been completely verified in thin sections yet.

Exact *P-T* conditions are difficult to establish by using the mineral assemblages described above. Investigations of the Bündnerschiefer and associated metabasites of the Lower Engadine Window by Bousquet et al. (1998, 2002, 2004) reveal a clear high-*P*-low-*T* history with *P-T* estimates ranging between 1.1–1.3 GPa and temperature around 350–375 °C, based on the occurrence of carpholite. However, indication of the high-*P*-low-*T* metamorphic assemblages in the metabasites are rare. Crossite (Na-amphibole, now discarded from IMA amphibole classification) and lawsonite occur in metabasites (Leimser and Purtscheller, 1980), and Mg-pumpellyite in association with chlorite, albite, and phengite occurs in metapelites. The *P-T* conditions calculated by Bousquet et al. (1998) for the upper units of the Lower Engadine Window are ca. 0.6 GPa and 300 °C. The Neoalpine metamorphism (data from the Tauern Window: 40–30 Ma, Schmid et al., 2013; Zimmermann et al., 1994) of the rocks of the Lower Engadine Window has been studied mainly in the Idalp Ophi-


**Figure 4:** The Idalp Formation is well exposed near the eastern end of Lange Wand, resting on the Steinsberg Formation (location see Fig. 1b). View towards southwest.

olite of the Upper Penninic Nappes, and on rocks of the Lower Penninic Nappes (Leimser and Purtscheller, 1980). No data exist on the metamorphism on the sediments of the Fimber Zone (Middle Penninic Nappes) including the Steinsberg and Idalp Formations.

## 3. Location

The study area is located on the northern margin of the Lower Engadine Window that is a tectonic window in which Penninic units are exposed below the Austroalpine nappes. The study area is in the Idalpe skiing area in the western Samnaun Mountain Group (Tyrol), between the Fimba Valley in the west and Bürkelkopf - Flimspitze in the east, approximately 5 km southeast of Ischgl (Fig. 1a, b), because it provides good exposures of both, the sedimentary rocks of the Steinsberg and Idalp formations and the Idalp ophiolite. We studied the magmatic rocks of the Idalp ophiolite in the eastern part of the area at the base of the Bürkelkopf massif near Velilljoch (Fig. 1b) and along the trail to Flimjoch. The sedimentary rocks were studied at the northern side of Greitspitze (2871 m), SW of Idjoch and near the eastern end of Lange Wand W of Idjoch (Fig. 1b).

## 4. Material and analytical methods

Rock samples were collected from a) sedimentary rocks of the Jurassic Steinsberg Formation that is composed of carbonate rocks, and Idalp Formation that is composed of siliciclastic sediments. We studied the Steinsberg Formation on the northern side of Greitspitze where we measured an almost complete section and collected 25 samples. Additional samples from the Steinsberg Formation were collected at the eastern end of Lange Wand and from the type locality Steinsberg near Ardez (Engadine, Switzerland). We measured a stratigraphic section through the Idalp Formation near the eastern end of Lange Wand where we collected eight sandstone samples. From all samples thin sections were prepared for the petrographic analysis of the sandstones and microfacies analysis of the carbonate rocks. Limestones were classified after Dunham (1962) and Embry and Klovan (1971). Rock samples were collected from the Idalp ophiolite including metagabbro and radiolarite (Velilljoch) and pillow-basalt (along the trail to Flimjoch). From selected samples (metagabbros, pillow basalts and a carbonate rock) polished thin sections were prepared for electron microprobe analyses (Fig. 1b).

Electron probe microanalysis (EPMA) was done using the JEOL 8100 SUPERPROBE at the Institute of Mineralo-

gy and Petrography at the University of Innsbruck. Analytical conditions were 15 kV and 10 nA sample current. Counting times for the measurements were 20 s on the peak and 10 s on the backgrounds. The following standards (standardized element in parenthesis) were used: jadeite (Na), orthoclase (K, Si), rutile (Ti), rhodonite (Mn), diopside (Ca), MgO (Mg), chromite (Cr), almandine (Fe), and corundum (Al).

Geothermobarometry using the multi-equilibrium method was done on metagabbro samples AF3b (dike in metagabbro) and AF17b (metagabbro) using the mineral assemblage amphibole + chlorite + albite + pumpellyite + quartz ± muscovite ± clinopyroxene to determine the maximum pressure/temperature conditions of these rocks during metamorphism during the Neoalpine orogeny. Most calculations were done without clinopyroxene, since it was not entirely clear if it belongs to the metamorphic phase assemblage, or still represents a magmatic relict. Mineral formula calculations were carried out with the program AX2 from the THERMOCALC v.3.33 program package using the thermodynamic dataset of Holland and Powell (1998, 2011). The AX2 program then calculates the activities of the individual phase components. All calculations were carried out in the $Na_2O$-CaO-FeO-MgO-$Al_2O_3$-$SiO_2$-$H_2O$ (NCFMASH) system. Two modes of calculations were done: Mode-1 calculates an invariant point in each chemical sub-system and Mode-2 the *averagePT* approach. In *averagePT*, the thermodynamics of an independent set of reactions between the endmembers of the mineral assemblage is combined statistically (by "least squares") to give a *P-T* result. *AveragePT* is the *P-T* point that is as "close" as possible (in a least-squares sense) to every reaction line (Powell and Holland, 2006). The effect of a change in water activity (water activity of 0.3; 0.5 and 0.7) on the obtained *P-T* conditions was investigated in sample AF3b. But due to the lack of constraints on $aH_2O$ all *P-T* calculations were done using $aH_2O$ of 1. For sample AF3b, in addition to the geothermobarometric calculations, the results were examined as a function of the water activity in the source rock ($aH_2O$ of 0.3, 0.5 and 0.7). The calcite-dolomite solvus geothermometer was used for the Idalp Formation carbonaceous sandstone sample AF29 using the calibration of Anovitz and Essene (1987).

## 5. Sedimentary Rocks of the Fimber Zone (Middle Penninic Nappes)

### 5.1. Steinsberg Formation

Other names are Steinsberger Kalk (Gürler and Schmutz, 1995; Gruber et al., 2010) or Lias in Steinsberger Fazies (Cadisch, 1932). Fuchs and Oberhauser (1990) mapped the Steinsberger Kalk at a scale of 1:50 000. Therefore, this lithostratigraphic unit is a mappable unit of Formation-rank and the term Steinsberg Formation is used.

#### *5.1.1. Steinsberg Formation, Greitspitze*

We studied the Steinsberg Formation at the northern side of Greitspitze (2871 m) where an almost complete succession is well exposed along a ski trail at an elevation of approximately 2730 m (Figs. 1b, 2, 3). The lowermost part of the Steinsberg Formation and the contact to the underlying strata as well as the contact to the overlying strata are not exposed (covered by talus slope). The contact to the overlying Idalp Formation is well exposed a few hundred meters farther north, near the eastern end of Lange Wand (Figs. 4, 5). The Steinsberg Formation at Greitspitze can lithologically be divided into a lower Brachiopodenkalk-Member that is overlain by the Crinoidenkalk-Member (Figs. 2, 3).

#### *5.1.2. Brachiopodenkalk-Member*

The Brachiopodenkalk-Member is approximately 19 m thick and composed of dark gray, bedded limestone with bed thickness of mostly 10–50 cm. Individual beds contain cm-large shell fragments of brachiopods and rare other fossils. Crinoidal debris is common. Although all sedimentary rocks are metamorphosed (and technically the limestones are marbles), the sediments are well preserved and limestone of the Brachiopodenkalk–Member is composed of the following microfacies types: Crinoidal packstone to rudstone, crinoid–brachiopod wackestone to packstone, crinoid–brachiopod wackestone to floatstone (Fig. 6a, b). In crinoidal packstone to rudstone echinoderm fragments (dominantly crinoids) are the most abundant grain type. Less abundant are shell fragments derived from brachiopods. Present in small amounts are benthic foraminifers. Ostracods, gastropods, bryozoans, echinoid spines and calcisponges are rare. Some of the fossil fragments, particularly shell fragments are partly silicified. Individual beds contain small amounts of detrital quartz grains and rare feldspar grains (grain size ca. 0.1 mm). The packstone to rudstone is locally well washed and cemented, locally contains small amounts of micritic matrix. In crinoid-brachiopod wackestone to packstone again crinoid and brachiopod fragments are the dominant grain types. Other fossils such as foraminifers, ostracods and gastropods are rare. This microfacies contains micritic matrix. Crinoid-brachiopod wackestone to floatstone has a similar composition but is coarser grained. In some of the limestone beds, brachiopod shells are more abundant than echinoderm (crinoid) fragments. The limestone near the top under the microscope appears as mixed siliciclastic–carbonate sandstone (Fig. 6c). This sandstone contains abundant detrital quartz grains (mostly 0.1–0.2 mm in diameter), dominantly monocrystalline, rare polycrystalline quartz, rare muscovite, many micritic rock fragments, rare phosphoritic rock fragments. The sandstone contains abundant echinoderm (crinoid) fragments and shell fragments of brachiopods, few foraminifers, echinoid spines and indeterminable skeletons.

### *5.1.3. Crinoidenkalk-Member*

The exposed thickness of the Crinoidenkalk-Member is approximately 36 m. The succession is composed of light-gray, medium to thick bedded, partly indistinctly bedded to massive limestone containing abundant crinoid fragments (encrinite) throughout the succession. In the upper part, individual beds contain crinoid stem fragments that are up to several cm long. Limestone in the lower part (basal 6–7 m; samples GRS 16, 17) is composed of crinoidal wackestone to packstone. Above limestone is composed of crinoidal grainstone, packstone and rudstone (Fig. 6d, e). The most abundant fossil fragments of crinoidal wackestone to packstone are echinoderm (dominantly crinoid) fragments. Brachiopod shell fragments are common, other fossils such as benthic foraminifers, ostracods and bryozoans are rare. The limestone contains small quartz grains with diameters mostly ranging from 0.1 to 0.2 mm (up to about 5%) and small amounts of micritic matrix. Crinoidal grainstone, packstone and rudstone is commonly well sorted and well–washed and composed almost entirely of echinoderm (mainly crinoid) fragments. Other fossils such as brachiopod shells, benthic foraminifers, ostracods, gastropods, echinoid spines and bryozoans are rare. In crinoidal grainstone echinoderm (crinoid) fragments constitute 65–70% of the rock, other fossils 0–5% and carbonate cement 30%. Most of the studied samples contain detrital quartz grains which in individual beds may constitute up to 40% of the rock. Also present are micritic intraclasts. One sample contains abundant well-rounded, dark brown micritic sedimentary rock fragments. Rarely thin layers (ca. 1 mm) containing abundant small (mostly 0.1–0.2 mm) detrital quartz grains are intercalated.

## 5.2. Idalp Formation

At the eastern end of Lange Wand, limestone of the Steinsberg Formation is overlain by 11 m of dark gray schist (Figs. 4, 5, unit 1) with few, thin intercalated fine-grained sandstone beds (1 cm). These schists are assigned to the Posidonienschiefer (*Posidonia* shale). Above follow interbedded schists and sandstones and two thin calcareous beds (5 and 10 cm thick) (Idalp-Sandstein sensu Oberhauser). Sandstone beds range in thickness from a few mm to 2 m. Sandstone beds are mostly fine- to medium-grained, thicker sandstone beds (Fig. 5, units 6 and 8) are partly coarse-grained. Most of the sandstone beds are micaceous. Thicker sandstone beds are partly laminated, mostly appear massive. Sandstone bed of unit 25 displays flaser bedding. The contact to the overlying sediments (Bunte Bündnerschiefer) is probably of tectonic origin (fault). Under the microscope sandstone is moderately to poorly sorted and composed of angular to subangular grains. Sandstone is composed of monocrystalline quartz (6–17%), polycrystalline quartz (14–29%), detrital feldspar grains including potassium feldspars and plagioclase (Fig. 6g, h). Feldspars are commonly altered to phyllosilicates to various degrees, and partly replaced

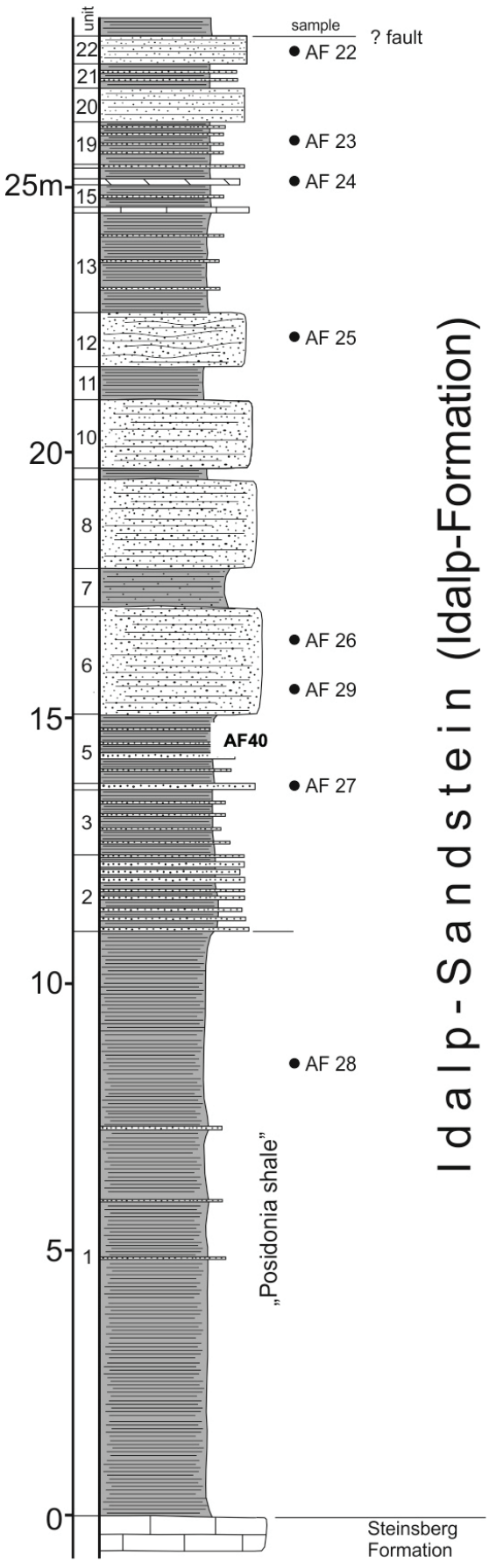


**Figure 5:** Stratigraphic section through the Idalp Formation, exposed near the eastern end of Lange Wand (location see Fig. 1b).

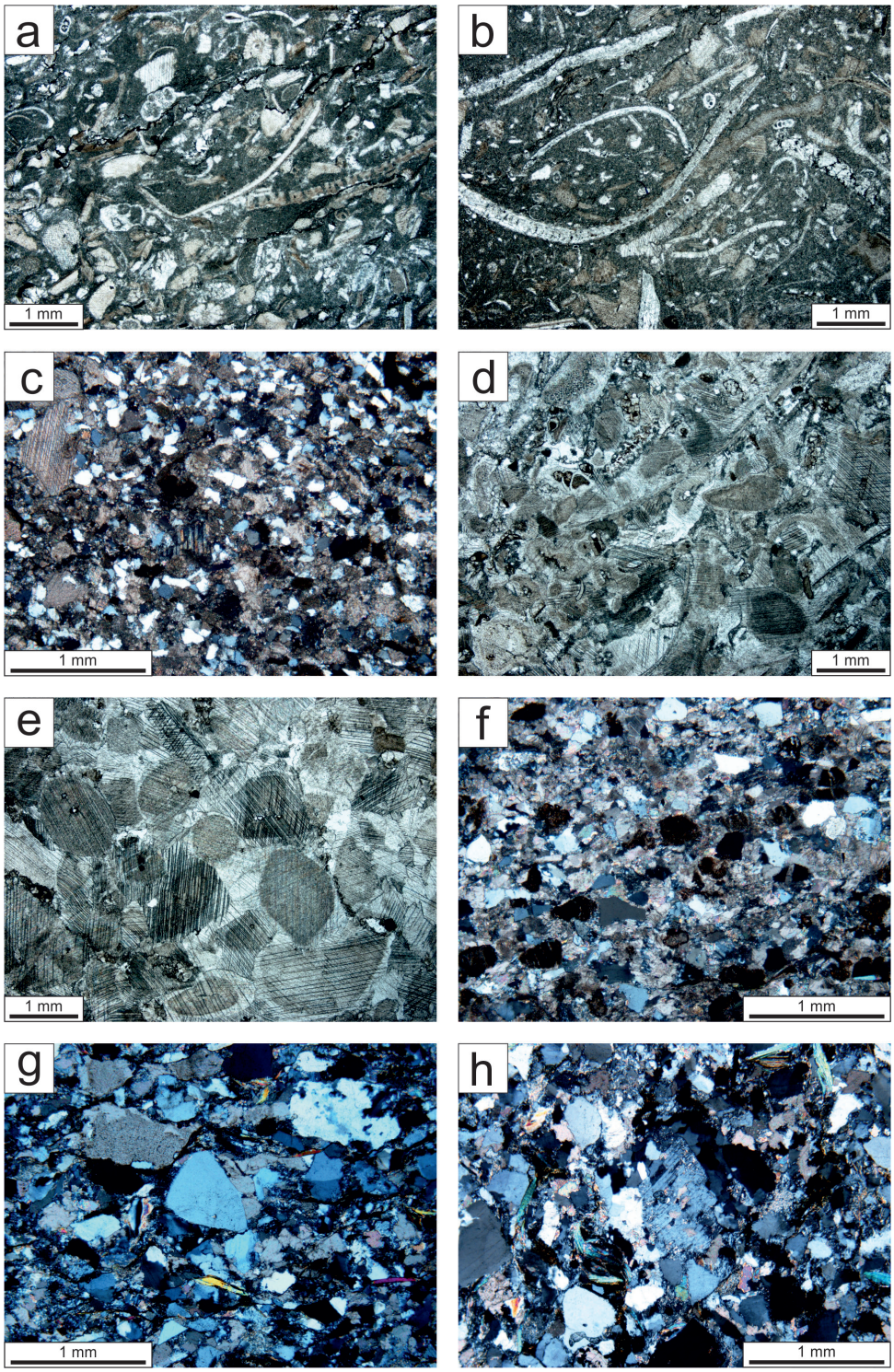


**Figure 6.** Thin section photographs of metasediments of the Steinsberg (a-e) and Idalp formations (f–h). (a), (b), (d) and (e) under non-polarized light; (c), (f–h) under polarized light. **(a)** Bioclastic wackestone to floatstone containing fragments of echinoderms (crinoids), ostracods, few foraminifers, punctate brachiopods and recrystallized micritic matrix. Sample AF20. Brachiopodenkalk-Member. **(b)** Bioclastic wackestone to floatstone containing abundant fragments of brachiopods and echinoderms (crinoids), recrystallized shell fragments (bivalves?), ostracods and rare foraminifers, embedded in recrystallized micritic matrix. Sample GRS 10, Brachiopodenkalk-Member. **(c)** Mixed siliciclastic-carbonate sandstone composed of abundant quartz grains, micritic intraclasts and echinoderm fragments. Sample GRS 10, Brachiopodenkalk-Member. **(d)** Packstone composed of abundant echinoderm (crinoid) fragments, few shell fragments of brachiopods and bivalves (?), ostracods and foraminifers. Sample GRS 16, base of Crinoidenkalk-Member. **(e)** Crinoidal grainstone to packstone, well-washed, composed almost entirely of crinoid fragments, many displaying syntaxial overgrowths. Sample GRS 22, Crinoidenkalk-Member. **(f)** Mixed siliciclastic-carbonate sandstone composed of abundant brownish to dark brownish carbonate rock fragments, mono- and polycrystalline quartz grains, few feldspar grains and rock fragments of quartz and feldspar. Sample AF24, Idalp Formation. **(g)** Sandstone composed of angular to subangular grains including mono- and polycrystalline quartz, subordinately feldspar, rock fragments of quartz and feldspar, muscovite and few echinoderm fragments (upper left). Sample AF22, Idalp Formation. **(h)** Sandstone, moderately sorted, composed of mono- and polycrystalline quartz grains, few feldspars, rock fragments including granitic rock fragments (large grain in the center), muscovite and calcite cement. Sample ID7, Idalp Formation.

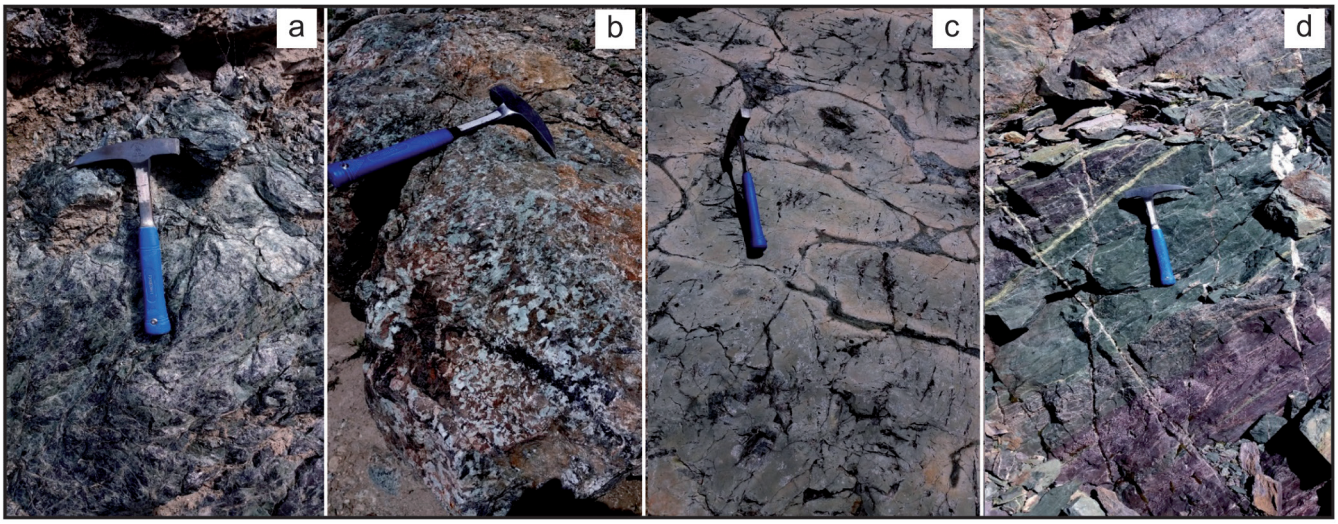


**Figure 7:** Outcrop photos of **(a)** serpentinite; **(b)** metagabbro, exposed near Velilljoch (MB on Fig. 1b); **(c)** pillow-basalt with well-preserved pillows and **(d)** greenish and reddish radiolarite exposed at Velilljoch.

by calcite (3–5%). Additional grain types are metamorphic and probably magmatic (granitic) rock fragments (Fig. 6h) composed of quartz and feldspar (gneiss, granitic), quartz and mica (schistose; metamorphic), micas (schistose, metamorphic) constituting 8–25%. Brownish sedimentary rock fragments (Fig. 6f) are composed of microcrystalline carbonate (0–18%), mica (muscovite; 1–3%). Fossil fragments are mainly represented by echinoderms (0–2%) (Fig. 6g). The sandstone contains blocky carbonate cement (mainly calcite, locally small amounts of dolomite; 15–45%) replacing detrital grains, particularly quartz and feldspars, and matrix (2–7%). Due to the high amount of rock fragments and low amount of detrital feldspar grains the sandstones are classified as lithic arenites after the classification scheme of Pettijohn et al. (1987).

The calcareous sandstone bed of unit 12 (Fig. 5) is composed of micritic to microsparitic matrix in which angular to subangular siliciclastic grains including mono- and polycrystalline quartz, metamorphic rock fragments, mica (muscovite), rare feldspar grains and abundant recrystallized fossil fragments are embedded. Fossils are represented by echinoderm fragments, shell fragments of brachiopods and probably bivalves, ostracods, rare foraminifers and undeterminable skeletal grains. Siliciclastic grains constitute 20 % of the calcareous sandstone, echinoderm fragments 5 % and other fossils 6.5 %. The thin calcareous sandstone bed of unit 4 in the middle of the succession is composed of coarse-grained recrystallized calcite in which siliciclastic grains such as mono- and polycrystalline quartz, metamorphic rock fragments, micas (muscovite) and rare feldspar grains are embedded. Echinoderm fragments may also be present but are difficult to determine.

## 6. Field relations and petrography of the metamorphic rocks of the Bürkelkopf Nappe (Upper Penninic Nappes)

### 6.1. Field relations

The serpentinites occur as highly fractured black to dark green rocks with a silver luster and crystal shapes of the protolith mineralogy are still visible (Fig. 7a). Occasionally, rodingite layers occur. The metagabbros are greenish to grey in color, coarse-grained and magmatic clinopyroxenes are still visible on the surface (Fig. 7b). The former plagioclase domains show white to greenish colors while the clinopyroxene domains are brown. The pillow basalts occur yellow to greenish whereby the rims of the pillows appear bleached (Fig. 7c). The inter-pillow spaces are dark green (Fig. 7c). The radiolarites are fine-grained, strongly foliated and show mostly green and red colors (Fig. 7d).

### 6.2. Petrography

Serpentinite is composed of colorless serpentine minerals (antigorite), dark brown relics of spinel and black magnetite crystals (Fig. 8a). The metagabbro contains abundant large clinopyroxene crystals in a very fine-grained matrix consisting of albite + muscovite + pumpellyite + epidote as shown in a photomicrograph in Figure 8b and in a BSE image in Figure 9a. The BSE image shows the fine-grained matrix of albite + muscovite + chlorite, which contains abundant epidote-bearing veins and from the textures it is not entirely clear, if clinopyroxene coexists with pumpellyite + amphibole + chlorite + magnetite as shown in Figure 9b. In metagabbro sample, AF17b, a large hornblende crystal occurs in a fine-grained matrix, while most amphiboles (tremolite to hornblende) are dispersed within the matrix (Fig. 9c). The pillow basalts also contain large clinopyroxene crys-

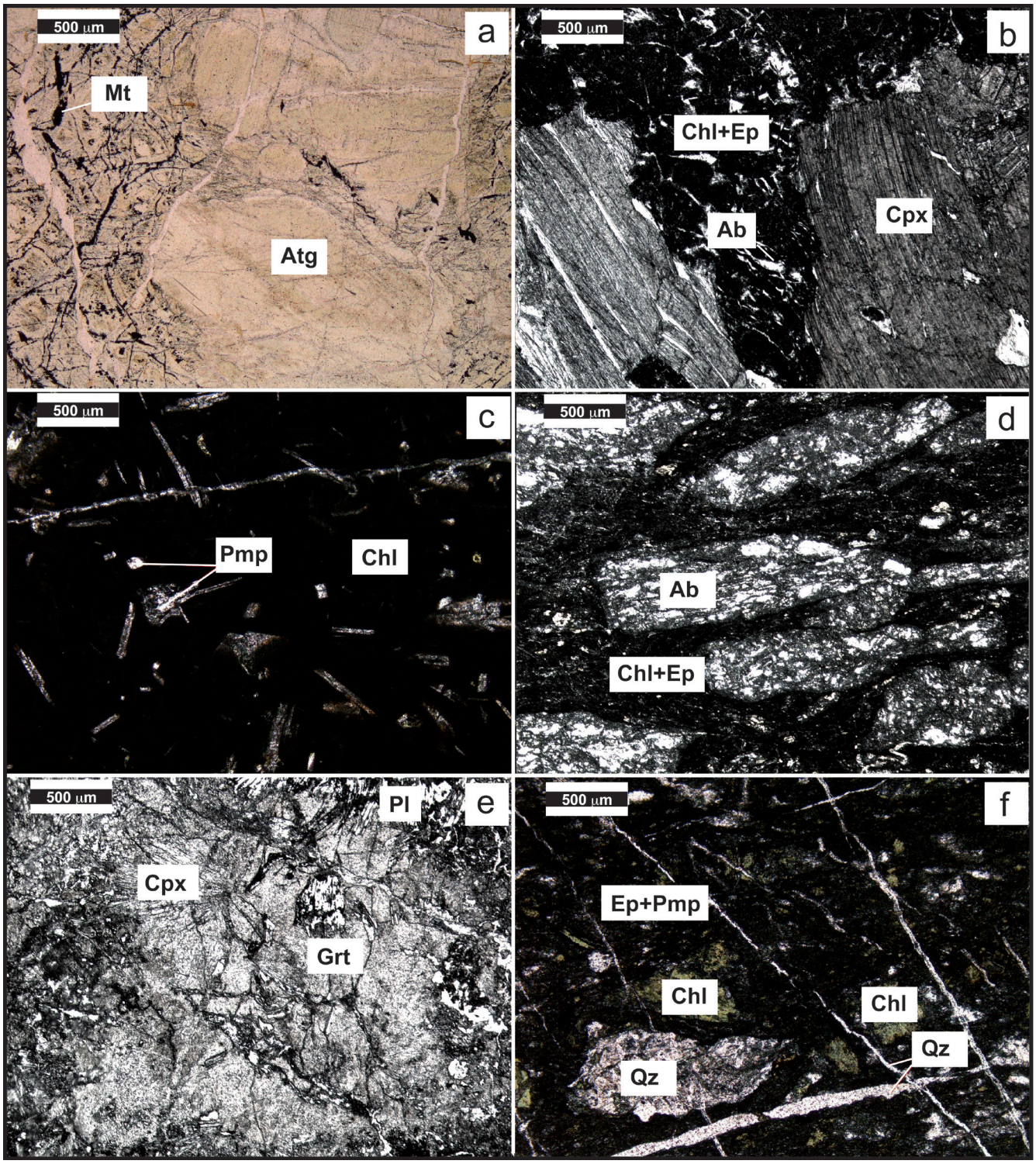


**Figure 8:** Photomicrographs of **(a)** serpentinite (sample AF1), which shows antigorite and black magnetite crystals. **(b)** metagabbro (sample AF17b) with large clinopyroxene crystals in a very fine-grained matrix consisting of albite + chlorite + epidote. **(c)** pillow basalt (sample AF14) containing clinopyroxene crystals in a very fine-grained almost black matrix consisting of pumpellyite + chlorite + albite + amphibole + titanite. (d) former plagioclase domain in pillow basalt containing albite. **(e)** rodingite, which consists mainly of clinopyroxene crystals in a fine-grained matrix of albite, muscovite and epidote. **(f)** radiolarites with the fine-grained mineral assemblage is chlorite + pumpellyite + epidote + titanite + oxides + albite + quartz (sample AF11). Mineral abbreviations: Atg: antigorite, Grt: garnet, Chl: chlorite, Ab: albite, Ep: epidote, Cpx: clinopyroxene, Pmp: pumpellyite, Amp: amphibole; Ttn: titanite; Pl: plagioclase; Qz: quartz.

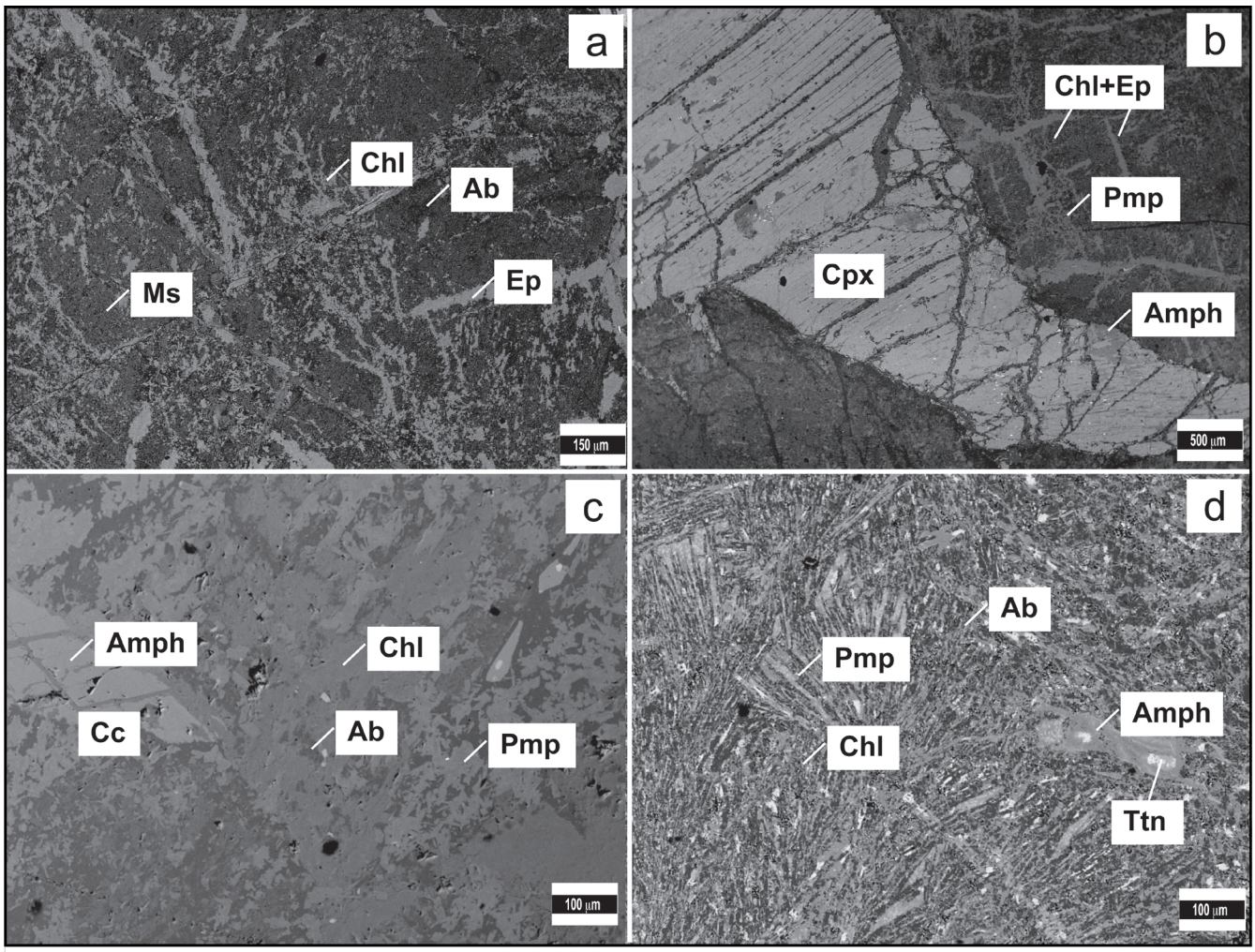


**Figure 9:** Backscattered electron (BSE) images of metagabbro (a–c, sample AF3b) and pillow basalt (d, sample AF14). **(a)** metagabbro showing the fine-grained matrix of albite + muscovite + chlorite with abundant epidote-bearing veins. **(b)** metagabbro with the assemblage clinopyroxene (probably relict) + pumpellyite + amphibole + chlorite + magnetite. **(c)** large amphibole in fine-grained matrix of albite + chlorite + pumpellyite in a metagabbro. **(d)** the fine-grained matrix in a pillow basalt sample can only be discerned using a close-up BSE image, which shows of the fine-grained matrix of pumpellyite + albite + chlorite + amphibole + titanite.

tals in a very fine-grained almost black matrix consisting of pumpellyite + albite + amphibole + titanite as shown in Figures 8c and 8d. The fine-grained matrix can only be discerned using BSE images, which reveal the assemblage pumpellyite + albite + amphibole + titanite. Figure 9d shows a BSE close up image of the fine-grained matrix of pumpellyite + albite + amphibole + titanite. Calcite + albite + epidote-bearing veins often crosscut the matrix. The rodingite (sample AF8) consists mainly of coarse-grained clinopyroxene crystals in a fine-grained matrix of albite, muscovite and epidote (Fig. 8e). Additional minerals are pumpellyite, stilpnomelane, garnet, amphibole, clinozoisite, titanite, prehnite, clinochlore and chalcopyrite. The radiolarites show an extensive foliation and vary in color from dark red/brown to green. This color variation also occurs within but also across the foliation. Abundant epidote rich veins crosscut the foliation. The mineral assemblage is chlorite + pumpellyite + epidote + titanite + oxides + albite + quartz (Fig. 8f). One calcareous sandstone sample from the Idalp Formation was investigated using BSE images, which revealed the mineral assemblage calcite + dolomite + apatite + quartz (Fig. 10a). For geothermometric considerations it was necessary to investigate if chemical zoning occurs in the calcite and a Mg-distribution map was done using the EPMA. The X-ray distribution map of Mg in Figure 10b clearly shows that calcite is chemically zoned and that dolomite inclusions coexist with the cores of Mg-bearing calcite (Cc-1) rimmed by Mg-free calcite (Cc-2), which later overgrew Cc-1.

### 6.3. Mineral chemistry

Chemical analyses of minerals were carried out on thin sections AF3b, AF7, AF17b, D1 and D2A. Representative chemical analyses of samples AF3b, AF17b and D2A are shown in Table 1. Mineral formula calculations were carried out with the program AX2 from the THERMOCALC

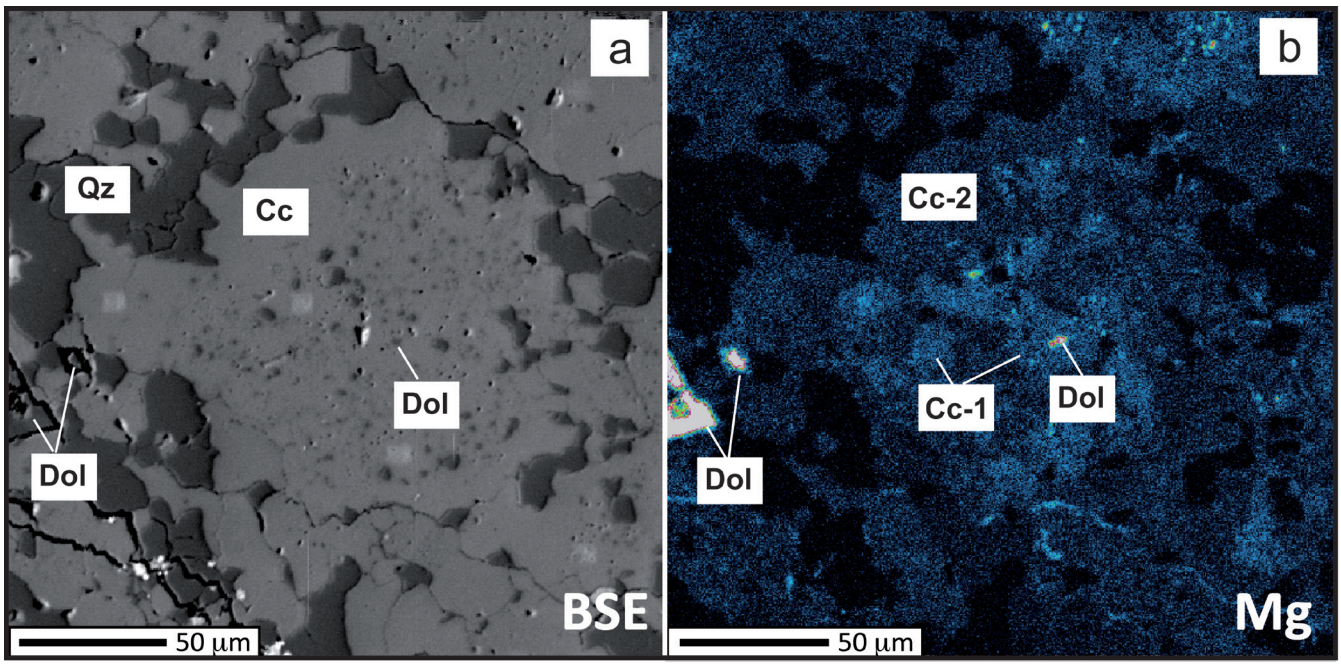


**Figure 10: (a)** The mineral assemblage calcite + dolomite + quartz from the calcareous Steinsberg Formation sandstone sample AF29. **(b)** shows the Mg-distribution image of **(a)** indicating that dolomite inclusions coexist with Mg-bearing calcite cores (Cc-1). The outer rim of calcite is composed of Mg-free calcite (Cc-2). Mineral abbreviations are the same as in Figure 8 in addition: Ms: muscovite; Cc: calcite, Dol: dolomite.

v.3.33 program package. The albite content of all samples is >88% and thus the feldspars are almost pure albites. Minor impurities such as MgO reach approx. 0.6 to 1.0 wt.% (sample D2A), while most analyses show very low contents of <0.2 wt.%. Chlorites have noteworthy average concentrations of minor elements of 0.27 wt.% MnO, 0.81 wt.% CaO and 0.14 wt.% $Cr_2O_3$ (sample AF3b). The chlorites can be classified as clinochlores. Muscovite in sample AF17b shows elevated Si contents of 3.44–3.52 apfu. The composition of many amphiboles shows a prograde chemical zonation with early growing tremolite/actinolite cores followed by hornblende in the outer rims and thus in samples AF3b and AF17b Mg-hornblende and occasional pargasite occur. Amphiboles show $TiO_2$ contents of up to 2.7 wt.%. The chemical compositions of the pumpellyite are like that of the pumpellyite-(Al) and most Fe is calculated as $Fe_2O_3$. The clinopyroxenes show FeO contents of up to 7.6 wt.%. All clinopyroxenes examined are augitic in composition. Clinopyroxenes show some chemical variation in their Na, Al and Ti contents. The Mg-content of relict calcite cores (Cc-1) of the Idalp Formation carbonaceous sandstone is 0.014–0.022 apfu (Tab. 3).

## 7. Geothermobarometry

Multi-equilibrium geothermobarometry using Mode-1 calculations yields up to four stable invariant points within the assemblage amphibole + albite + chlorite + quartz + pumpellyite ± muscovite for two metagabbro samples (AF3b, AF17b). For Mode-1 *P-T* estimation the invariant point with the phase components clinochlore + diopside + quartz + tremolite + anorthite + pargasite + albite + $H_2O$ was selected. The Mode-1 *P-T* calculations yield pressures of 0.63 to 0.95 GPa and temperatures between 330 °C and 390 °C. Due to the restricted chemical system of the invariant points and the use of linearly dependent reactions, these results are only of semi-quantitative nature. The more robust Mode-2 calculations of samples AF3b and AF17b yields *P-T* conditions of 0.80 ± 0.14 GPa and 355 ± 21 °C (sigfit = 0.09, sample AF3b) and 0.74 ± 0.13 GPa and 350 ± 19 °C (sigfit = 0.80, sample AF17b) as shown in Table 4. Since it is not entirely clear, if clinopyroxene represents a relict magmatic phase, or recrystallized during the metamorphic event additional Mode-2 calculations were done including clinopyroxene (see Tab. 4). These calculations yield virtually identical *P-T* conditions of 0.75 ± 0.14 GPa and 350 ± 19°C (sigfit = 1.14, sample AF3b) and 0.70 ± 0.14 GPa and 343 ± 22 °C (sigfit = 1.15, sample AF17b) indicating that clinopyroxene might have recrystallized during the Neoalpine event. It can also be shown that the *P-T* results strongly depend on different $aH_2O$ as shown for sample AF3b in Table 2. The following Mode-1 invariant point is used for these calculations:

clinochlore + 5diopside +5quartz = 2tremolite + anorthite + $2H_2O$
pargasite + diopside + 5quartz = tremolite + anorthite + albite
clinochlore + anorthite + 2albite + 3diopside = 2 pargasite + 5quartz + $2H_2O$

| Sample | AF3b | AF3b | AF3b | AF3b | AF3b | AF3b | AF17b | AF17b | AF17b | AF17b | AF17b | D2A | D2A | D2A | D2A |
|---|---|---|---|---|---|---|---|---|---|---|---|---|---|---|---|
| Mineral | amp | amp | chl | pmp | fsp | cpx | mu | amp | ab | chl | pmp | pmp | fsp | cpx | chl |
| $SiO_2$ | 46.00 | 49.86 | 31.54 | 38.76 | 68.39 | 52.86 | 53.53 | 50.46 | 67.00 | 31.47 | 37.36 | 37.77 | 66.39 | 51.02 | 29.67 |
| $TiO_2$ | 2.71 | 1.01 | 0.03 | 0.12 | n.d. | 0.45 | 0.04 | 0.96 | n.d. | 0.05 | 0.01 | 0.08 | 0.74 | 1.47 | 0.03 |
| $Al_2O_3$ | 8.73 | 5.57 | 18.33 | 23.16 | 19.07 | 2.34 | 26.56 | 4.61 | 18.65 | 15.8 | 25.04 | 22.45 | 18.22 | 2.99 | 17.33 |
| $Cr_2O_3$ | 0.13 | 0.14 | 0.25 | 0.20 | n.d. | 0.08 | n.d. | 0.09 | n.d. | 0.13 | n.d. | 0.12 | n.d. | 0.12 | 0.04 |
| $Fe_2O_3$ | 0.98 | 4.33 | n.d. | 3.63 | 0.32 | n.d. | n.d. | 1.52 | 0.7 | n.d. | 1.31 | 5.71 | 1.53 | 7.06 | n.c. |
| FeO | 9.37 | 7.77 | 12.49 | 0.36 | n.d. | 7.07 | 1.11 | 6.04 | n.d. | 14.19 | 2.05 | 1.86 | n.d. | 9.27 | 21.09 |
| MnO | 0.15 | 0.30 | 0.22 | 0.19 | n.d. | 0.27 | n.d. | 0.16 | n.d. | 0.19 | 0.20 | 0.29 | 0.05 | 0.39 | 0.34 |
| MgO | 14.84 | 15.74 | 20.64 | 4.22 | 0.06 | 15.91 | 2.44 | 19.71 | 0.65 | 23.72 | 1.94 | 2.41 | 0.94 | 9.81 | 18.12 |
| CaO | 11.67 | 10.29 | 4.17 | 21.96 | 0.34 | 20.00 | 0.19 | 11.31 | 0.39 | 0.5 | 22.43 | 22.46 | 1.33 | 14.95 | 0.42 |
| $Na_2O$ | 2.01 | 1.54 | 0.03 | 0.09 | 11.33 | 0.40 | 2.05 | 1.50 | 11.38 | 0.06 | 0.21 | 0.08 | 10.81 | 3.43 | 0.18 |
| $K_2O$ | 0.35 | 0.08 | 0.01 | 0.01 | 0.18 | 0.04 | 9.19 | n.d. | 0.33 | 0.04 | 0.09 | 0.02 | 0.04 | 0.04 | n.d. |
| Total | 96.94 | 96.63 | 87.71 | 92.70 | 99.69 | 99.42 | 95.11 | 96.38 | 99.10 | 86.15 | 90.55 | 93.25 | 100.05 | 100.55 | 87.22 |
| Si | 6.716 | 7.216 | 3.115 | 6.192 | 2.999 | 1.954 | 3.532 | 7.232 | 2.971 | 3.167 | 6.122 | 6.108 | 2.931 | 1.917 | 3.063 |
| Ti | 0.298 | 0.110 | 0.002 | 0.014 | n.d. | 0.013 | 0.002 | 0.103 | n.d. | 0.004 | 0.001 | 0.010 | 0.025 | 0.042 | 0.002 |
| Al | 1.503 | 0.950 | 2.135 | 4.362 | 0.986 | 0.102 | 2.066 | 0.779 | 0.975 | 1.875 | 4.838 | 4.280 | 0.948 | 0.132 | 2.109 |
| Cr | 0.015 | 0.016 | 0.020 | 0.025 | n.d. | 0.002 | n.d. | 0.01 | n.d. | 0.01 | n.d. | 0.015 | n.d. | 0.004 | 0.003 |
| $Fe^{3+}$ | 0.108 | 0.472 | n.d. | 0.436 | 0.011 | n.d. | n.d. | 0.164 | 0.023 | n.d. | 0.161 | 0.695 | 0.051 | 0.200 | n.c. |
| $Fe^{2+}$ | 1.144 | 0.941 | 1.032 | 0.048 | n.d. | 0.219 | 0.061 | 0.724 | n.d. | 1.194 | 0.281 | 0.252 | n.d. | 0.291 | 1.821 |
| Mn | 0.019 | 0.037 | 0.018 | 0.026 | n.d. | 0.008 | n.d. | 0.019 | n.d. | 0.016 | 0.028 | 0.040 | 0.002 | 0.012 | 0.030 |
| Mg | 3.229 | 3.395 | 3.038 | 1.005 | 0.004 | 0.876 | 0.24 | 4.21 | 0.043 | 3.558 | 0.474 | 0.581 | 0.062 | 0.549 | 2.787 |
| Ca | 1.826 | 1.596 | 0.441 | 3.759 | 0.016 | 0.792 | 0.013 | 1.737 | 0.019 | 0.054 | 3.938 | 3.892 | 0.063 | 0.602 | 0.046 |
| Na | 0.569 | 0.432 | 0.006 | 0.028 | 0.963 | 0.029 | 0.262 | 0.417 | 0.979 | 0.012 | 0.067 | 0.025 | 0.925 | 0.250 | 0.036 |
| K | 0.065 | 0.015 | 0.001 | 0.002 | 0.010 | 0.002 | 0.774 | n.d. | 0.019 | 0.005 | 0.001 | 0.004 | 0.002 | 0.002 | n.d. |
| Sum | 15.491 | 15.179 | 9.809 | 15.897 | 4.989 | 3.997 | 6.951 | 15.396 | 5.028 | 9.895 | 15.911 | 15.902 | 5.009 | 4.000 | 9.897 |

**Table 1:** Representative electron probe microanalyses data of samples AF3b, AF17b and D2A. Mineral abbreviations: amp: amphibole, chl: chlorite, pmp: pmpellyite, cpx: clinopyroxene, fsp: feldspar; oxygen base of the mineral formula calculation: amphibole 23 O; chlorite 14 O, pumpellyite: 24.5 O, albite: 8 O, clinopyroxene: 6 O and muscovite: 11 O. n.d. not detected; n.c. not calculated.

| $a$H$_2$O | $P$(GPa) | 1σ | $T$(°C) | 1σ |
|---|---|---|---|---|
| 1.0 | 0.79 | 0.09 | 317 | 17 |
| 0.7 | 0.75 | 0.08 | 287 | 16 |
| 0.5 | 0.72 | 0.08 | 262 | 14 |
| 0.3 | 0.67 | 0.08 | 228 | 13 |

**Table 2:** The influence of $a$H$_2$O on *P-T* conditions of sample AF3b.

| | |
|---|---|
| Fe apfu | <0.001–0.004 |
| Mn apfu | <0.001 |
| Mg apfu | 0.014–0.022 |
| Ca apfu | 0.977–0.986 |
| *X*Mg (Cc) | 0.016–0.022 |
| $T$(°C) | 262–379 |

**Table 3:** Results of cc-dol geothermometry of sample AE29. *T* calculated using the calibration of Anovitz and Essene (1987); apfu: atoms per formula unit.

clinochlore + albite + 4diopside = tremolite + pargasite + 2H$_2$O

3tremolite + clinochlore + 4anorthite + 5albite = 5pargasite +20quartz + 2H$_2$O

The *P-T* conditions decrease from 0.79 GPa and 317 °C ($a$H$_2$O of 1.0) to 0.67 GPa and 228 °C ($a$H$_2$O of 0.3). The application of the calcite-dolomite geothermometer with the calibration of Anovitz and Essene (1987) to the carbonaceous sandstone of the Idalp Formation to relict Mg-bearing calcite cores (Cc-1) coexisting with dolomite (Fig. 10b) yields temperatures ranging from 262 to 379 °C (Tab. 3). The mean temperature is 330 ± 35 °C. These temperatures correlate very well with the temperatures from the multi-equilibrium calculations at high $a$H$_2$O as given above.

## 8. Discussion

### 8.1. Depositional environment of the Steinsberg- and Idalp formations

The Steinsberg Formation (Sinémurian - Toarcian) of the studied section at Greitspitze is divided into the lower Brachiopodenkalk-Member, overlain by the Crinoidenkalk-Member. The Brachiopodenkalk-Member is composed of crinoidal packstone to rudstone, crinoid-brachiopod wackestone to packstone and crinoid-brachiopod wackestone to floatstone that are interpreted as deposits of a shallow, low-energy shelf environment. The overlying Crinoidenkalk-Member, composed of a thick accumulation of mainly crinoid fragments ("encrinite") (mainly crinoidal packstone, grainstone and rudstone, rare wackestone) formed in a shallow, normal marine environment of moderate turbulence.

Crinoids are mostly sessile filter feeders indicating a depositional environment of nearly normal salinity. Mass accumulations (encrinites) of benthic crinoid elements are reported from different marine depositional environ-

ments ranging from shallow marine to deep marine settings. The Steinsberg Formation that is mainly composed of encrinites is widely distributed in the Fimber Zone and Tasna Nappe and thus may be regarded as a "regional encrinite" sensu Ausich (1997). According to Ausich (1997), "regional encrinites" were deposited below normal wave base but above the storm wave base. Due to their low density of 1.2 g/cm$^3$ crinoid fragments are easily transported even by weak currents over longer distances. The presence of larger stem fragments (up to about 10 cm long) in the encrinites of the Steinsberg Formation indicates that the crinoids were deposited in–situ and have not been transported over longer distances. Encrinites of Sinémurian–Pliensbachian age are widespread in the Northern Calcareous Alps where they are termed Hierlatzkalk. The Hierlatzkalk is a red to subordinately light gray encrinite that is 20–80 m thick composed of crinoidal packstone, partly wackestone with patchy accumulations of brachiopods (Tollmann, 1976; Böhm, 1986).

In encrinites of the Hierlatzkalk most of the crinoid fragments show traces of abrasion indicating transportation on the ground, display borings, and commonly the pores of the crinoid fragments are filled with micrite. Red impregnation indicates low sedimentation rates (Böhm, 1986). We did not observe these characteristics on the crinoid fragments in the encrinites of the Steinsberg Formation. According to Tollmann (1976) encrinites of the Hierlatzkalk represent the "Seichtschwellenfazies" (facies of shallow swells/highs) of the Liassic. The encrinites were deposited in shallow turbulent water. Böhm (1986) concludes that the encrinites of the Hierlatzkalk were deposited by currents on isolated highs (Schwellen) below the wave base. We interpret the deposits of the Brachiopodenkalk-Member of the Steinsberg Formation (very similar to the Lias–Brachiopodenkalk of the Northern Calcareous Alps; Tollmann, 1976) as deposits of a shallow, low energy shelf environment and the overlying Crinoidenkalk-Member (encrinites) as "regional encrinite" deposited in a shallow, normal marine environment of moderate turbulence.

Sedimentary rocks of the Idalp Formation do not provide clear indications for the depositional environment. The ichnofossil *Chondrites* is assigned to the *Cruziana* ichnofacies that is characteristic of a subtidal environment composed of poorly sorted or heterolithic, cohesive to semi–cohesive sediments (MacEachern et al., 2010). Depositional environments range from moderate–energy, shallow water below fair-weather wave base but above storm wave base to low–energy settings in deeper water with periods of high energy (storm deposits) (MacEachern et al., 2010). *Zoophycos* is a poorly understood ichnofossil. *Zoophycos* has an extremely broad paleodepositional range and occurs in the *Cruziana* through the *Nereites* ichnofacies (MacEachern et al., 2010). *Zoophycos* changed environments through geologic time. *Zoophycos* commonly occurs in shallow–marine deposits during the Paleozoic, but it became primarily a deep-sea trace from the Mesozoic onward (Miller, 1991; Zhang et al., 2015).

Oberhauser (1980, 1984) interpreted the Idalp Formation as flysch deposits ("Flysch mit Glimmersandsteinbänken"). Oberhauser (1976, 1980) compared the schists at the base of the Idalp Formation with the *Posidonia* shale. The *Posidonia* shale was deposited during the Toarcian Oceanic Anoxic Event (TOAE), a global anoxic event causing deposition of organic–rich sediments. We did not observe high amounts of organic material in the schists at the base of the Idalp Formation in the studied section. It is not clear if the fossils and ichnofossils mentioned by Oberhauser (1984) occur in the "*Posidonia* shale" or in schists interbedded in the sandstone (Idalp-Sandstein according to Oberhauser). The "*Posidonia* shale" sensu Oberhauser (1976, 1980) most likely formed during the Toarcian in an oxygen–depleted marine environment. The occurrence of *Chondrites* indicates deposition in a deeper shelf environment. Oberhauser (1984) interpreted the intercalated sandstone beds as turbidites. We did not observe typical features such as graded bedding or Bouma sequences in the studied section. Rock fragments of the sandstone that are composed of quartz and feldspars, quartz and micas, and muscovite are derived from metamorphic crystalline rocks. Bertle et al. (2003) reported Ar-Ar and Rb-Sr-ages of 270 Ma for micas of the Idalp Formation and 310 Ma for the Tasna granite. In Variscan times, a series of granitoids intruded the pre-Variscan basement, starting around 300 Ma and lasting until the middle Permian (Hunziker et al., 1992). The micas of the Idalp Formation are most probably derived from metamorphic basement rocks, which show Variscan metamorphic ages.

It must be emphasized that additional, detailed investigations are necessary for a better understanding of the depositional environment of the Idalp Formation. The succession of flysch-like dark brown to black schists with intercalated thin sandstone beds (including Bouma sequences) overlying the Steinsberg Formation near Ardez (Tasna Nappe) is similar in age and facies to the Idalp Formation of the Fimber Zone. Contemporaneous sandstones and schists occur in other Penninic units like in the Falknis Nappe (termed Panier Formation), Gelbhorn Nappe ("Dogger Sandstone"), Arosa Zone and Zone of Samaden (Gruner, 1981). The sharp lithologic boundary between the Steinsberg Formation and overlying Idalp Formation indicates a sudden deepening of the depositional environment coupled with increased siliciclastic influx that stopped carbonate production and caused deposition of shales in a probable oxygen depleted deeper shelf setting (Toarcian Oceanic Anoxic Event). Shallow marine carbonate shelf deposits of the Steinsberg Formation prevailed during most of the Lower Jurassic. Deepening of the depositional environment started during the Toarcian and continued until the Eocene (Waibel and Frisch, 1989).

According to Handy et al. (2010) the opening of the Piemont-Liguria Ocean occurred from 200–170 Ma (Lower to Middle Jurassic), whereas the opening of the Valais Ocean was from 131–93 Ma (Cretaceous; Hauteriv-

AF3b: independent set of reactions between amphibole + pumpellyite + albite + chlorite + quartz

33ts + 6pump + 19q = 10tr + 11clin + 70an
11fact + 33ts + 6pump + 19q = 21tr + 11daph + 70an
283ts + 48pump + 38ab = 61tr + 38parg + 88clin + 560an
3tr + clin + 4an + 5ab = 5parg + 20q + $2H_2O$

- $T$ = 355°C, 1σ = 21°C,
- $P$ = 0.8 GPa, 1σ = 0.14 GPa, sigfit = 0.09

AF3b: independent set of reactions between clinopyroxene + amphibole + pumpellyite + albite + chlorite + quartz

tr + 22clin + 102an + 38di = 47ts + 12pump
33ts + 6pump + 19q = 10tr + 11clin + 70an
43tr + 110clin + 510an + 190hed = 38fact + 235ts + 60pump
23tr + 22daph + 102an + 38di = 22fact + 47ts + 12pump
3tr + daph + 9an = 5ts + 5hed + 5q + $2H_2O$
283ts + 48pump + 38ab = 61tr + 38parg + 88clin + 560an

- $T$ = 348°C, 1σ = 24°C
- $P$ = 0.75 GPa, 1σ = 0.15 GPa, sigfit = 1.14

AF17b: independent set of reactions between amphibole + pumpellyite + albite + chlorite + muscovite + quartz

6pump + 33ts + 19q = 11clin + 70an + 10tr
88clin + 560an + 61tr + 38parg = 38ab + 48pump + 283ts
clin + 4an + 5ab + 3tr = 5parg + 20q + $2H_2O$
440cel + 88daph + 560an + 61tr + 38parg = 440fcel + 38ab + 48pump + 283ts

- $T$ = 350°C, 1σ = 19°C,
- $P$ = 0.74 GPa, 1σ = 0.13 GPa, sigfit = 0.80

AF17b: independent set of reactions between clinopyroxene + amphibole + pumpellyite + albite + chlorite + quartz

12pump + 47ts = 38di + 22clin + 102an + tr
66di + 11clin + 4an + 47q = 6pump + 23tr
6pump + 21ts = 19di + 10clin + 47an + $2H_2O$
10hed + 12pump + 47ts = 148di + 22daph + 102an + tr
30pump + 68tr + 47parg = 283di + 55clin + 67an + 47ab

- $T$ = 343°C, 1σ = 22°C,
- $P$ = 0.7 GPa, 1σ = 0.14 GPa, sigfit = 1.15

**Table 4:** Results of Mode-2 multi-equilibrium geothermobarometry. Mineral abbreviations: ts: tschermakite, tr: tremolite, clin: clinochlore, ab: albite, an: anorthite, di: diopside, pump: pumpellyite, parg: pargasite; hed: hedenbergite; daph: daphnite; fact: ferro-actinolite, cel: celadonite, fcel: ferro-celadonite, q: quartz. Sigfit: statistical measure for 95% confidence.

ian - Cenomanian). The beginning of the opening of the Piemont-Liguria Ocean during the Hettangian (Lower Jurassic) marks the beginning of the deposition of syn-rift sediments. Thus, both, Steinsberg and Idalp formations represent syn-rift deposits of the Iberia-Briançonnais microcontinent. In the Northern Calcareous Alps, the onset of the rifting processes caused breakdown of the Upper Triassic carbonate platforms and the formation of several pull-apart basins and structural highs, starting during the Hettangian (e.g. Bernoulli and Jenkyns, 1970; Böhm, 1986; Mostler and Krainer, 1993; Krainer et al., 1994). On the northern margin of the northwestern Calcareous Alps, a shallow carbonate platform prevailed until the Lower Jurassic, on which oolitic limestones (Geiselstein Oolith) were deposited, associated with crinoidal limestone (Fabricius, 1967). Limestones of the Steinsberg Formation indicate that also on the margin of the Iberia- Briançonnais microcontinent a shallow marine shelf existed during most of the Lower Jurassic.

### 8.2. The metamorphic evolution of the Idalp Ophiolite

The *P-T* results of metagabbro samples AF3b and AF17b indicate a regional metamorphic event at low-*T* conditions and low to medium-*P* conditions and thus correspond to the transition of the upper greenschist to lower blueschist facies. The obtained *P-T* conditions are similar to the results from Höck et al. (2004) of 350°C and 0.7–0.9 GPa but represent more robust *P-T* estimates since Mode-2 allows statistical treatment of the *P-T* data and we also evaluate the role of $a(H_2O)$ on the *P-T* results. Unfortunately, it is not possible to calculate pressures from the calcareous sandstone sample AF29 of the Idalp Formation, but the average temperature determined Mg-bearing calcite cores coexisting with dolomite is approx. 330 ± 25°C and thus well within the average temperatures of our multi-equilibrium results and the results of Höck et al. (2004). Two metamorphic events have overprinted the rocks of the Lower Engadine window: an older, possibly Jurassic oceanic high–temperature metamorphism and a younger Eocene high–pressure metamorphism (Höck et al., 2004; Schuster et al., 2004). Large hornblende crystals in sample AF17b provide evidence for the older Jurassic event (Fig. 4b), while metamorphic hornblendes grew as smaller crystals within the matrix adjacent to clinopyroxenes. Compared to the lower unit of the Penninic Bündner schists in the Lower Engadine Window (Mundin unit), however, the *P-T* conditions obtained in this study are significantly lower than the *P-T* conditions of Bousquet et al. (1998) of 1.1–1.3 GPa for a temperature around 350–375°C. However, our *P-T* results correlate very well with the *P-T* conditions of the upper Bündnerschiefer unit (Arina unit), as the degree of metamorphism in the Idalp ophiolite experienced only low to medium pressures. It is therefore possible that at the time of metamorphism the ophiolite complex was more in the hanging areas during the Neoalpine orogeny, compared to the lower Bündnerschiefer unit. In the metagabbros and gangue (AF3b, AF7, AF17b) large clinopyroxenes with amphibole growth on the rims can be observed (Mg-hornblende, pargasite to actinolite) as well as a somewhat uncertain metamorphic recrystallization of clinopyroxene in microdomains based on their diopside-rich magmatic compositions. On the other hand, the occurrence of clinopyroxene with such diopside-rich rather than omphacitic compositions has been reported from metagabbros (Corno et al., 2023). Light and dark areas in the clinopyroxenes in the BSE images may indicate this transformation since the lighter areas show higher Ca contents (magmatic?) and the darker areas may be interpreted as metamorphic recrystallized clinopyroxene with higher Na and Al contents, which is in perfect agreement with the *P-T* results from the Mode-2 calculations involving clinopyroxene. The presence of abundant chalcopyrite in sample AF7 indicates possibly hydrothermal conditions in connection with a sulphide-rich environment. It is therefore possible that the sulfidization formed in association with black smoker (VMS deposit type) activities during the older Jurassic oceanic high–temperature metamorphism. Chalcopyrites were also encountered at the contact between Steinsberg Limestone (Formation) and the Idalp Sandstone (Formation). Rodingites are associated with metagabbros in the rocks of the Idalp Ophiolite, which occur along metasomatic reactions at the contact between serpentinites and silicate-rich country rocks. In the pillow basalt sample (AF14), epidote-rich veins occur in the rock, while higher calcium contents occur in the primary albites. These are indicators of Ca-metasomatism, which is also represented by blackish red locally occurring oxidations (e.g. hematite) and coeval with rodingite formation in the metagabbros.

Concerning the prograde and retrograde metamorphic evolution of the Idalp Ophiolite during the Neoalpine orogeny the following can be stated: From the mid-Upper Cretaceous onwards, oceanic crust and lithosphere of the Piemont-Liguria and Valais oceans was subducted southwards beneath the Austroalpine units and pushed far onto the European shelf (Schmid et al., 2004). The degree of metamorphism of the Idalp ophiolite (upper Penninic unit) during the Neoalpine metamorphic event is classified as low temperature/high-pressure metamorphism. The pressure/temperature conditions are in the transition zone from the greenschist-facies to the blueschist-facies with 0.7–0.9 GPa at about 350°C (Koller, 1985; Höck et al., 2004). The peak mineral assemblage is pumpellyite + chlorite + albite + epidote + actinolite + muscovite + titanite + hematite ± clinopyroxene. The obtained geothermobarometric results of this work provide robust *P-T* data with realistic error estimates and are consistent with the results of Höck et. al. (2004) as well as Bousquet et al. (1998, 2002, 2004) and Leimser and Purtscheller (1980). According to Leimser and Purtscheller (1980), a prograde metamorphic zonation from the outer areas to the central part of the Lower Engadine Window is recognizable. The following metamorphic minerals were observed: Pumpellyite, lawsonite (3 outcrops), stilpnomelane and glaucophane (1 outcrop). From the breakdown of lawsonite and pumpellyite and the Formation of glaucophane, they derived maximum *P-T* conditions of 350°C and 0.4–0.5 GPa. The occurrence of pelitic high-*P*/low-*T* index minerals (carpholite, chloritoid) in the Mundin unit supports high-*P*/low-*T* metamorphism with higher pressures of 1.2–1.4 GPa and temperatures of about 350°C (Bousquet et al., 1998). These conditions are present in the central area of the Lower Engadine window, where the core of the anticline is located. In the Arina unit, pressure/temperature conditions of 300°C and 0.6 GPa were calculated in metapelites with the assemblage pumpellyite-(Mg), chlorite, albite and phengite (Bousquet et al., 1998). Comparing the *P-T-t* paths from Bousquet et al. (1998, 2002) and the geothermobarometric results from this study reveals that samples AF3b and AF17b show slightly higher temperatures in some cases than temperatures in the *P-T-t* paths from Bousquet et al. (1998) from the Mundin and Arina units of the Lower Engadine Window.

According to Höck and Koller (1989), lawsonite occurs locally in the Idalp ophiolite, which is typical of blueschist-facies metamorphism and occurs as a secondary mineral in an altered metagabbro. Furthermore, isolated blue amphiboles and high Si-phengitic mica are present in the metagabbro, which according to Schuster et al. (2004) also indicate blueschist-facies metamorphism. Despite the fact that these features only occur locally or rarely or sporadically in the work of Höck and Koller (1989) and not in the samples of this investigation (no lawsonite or glaucophane) could be due to kinetic factors and/or the lack of fluids. Nonetheless, the obtained *P-T* results indicate clearly that blueschist-facies metamorphism occurred pervasively throughout the Idalp ophiolite.

## 9. Conclusions

Petrographic and sedimentological investigations on numerous rock samples from the Lower Engadine Window provide new data on the composition and depositional environment of the Jurassic Steinsberg and Idalp formations of the Middle Penninic Nappes, on the Idalp ophiolite of the Upper Penninic Nappes, and on the Neoalpine regional metamorphism. The Steinsberg Formation is composed of carbonate sediments rich in crinoid fragments ("encrinites") that accumulated in a shallow, normal marine depositional setting on the shelf of the Iberia-Briançonnais microcontinent. Overlying sediments of the Idalp Formation, represented by shale and intercalated sandstone, are interpreted of a deeper marine shelf setting. Quantitative *P-T* data from the metagabbros of the Idalp ophiolite of the Upper Penninic Nappe system indicate that the rocks of the Idalp ophiolite (metagabbro, metabasalt, rodingite, radiolarite) underwent regional metamorphism at *P-T* conditions of 0.60–0.95 GPa and 330–390°C characteristic for the transition zone between greenschist- to blueschist-facies conditions in an accretional/subduction setting. This regional metamorphism is interpreted to be of Neoalpine age. For the first time *P-T* data are presented from a calcareous sandstone of the Idalp Formation of the Fimber Zone of the Middle Penninic Nappe system indicating low-*T* metamorphism. This high-*P*/low-*T* metamorphism is manifested not only in the ophiolite sequence but also in the overlying sediments and is related to Neoalpine subduction processes during the closure of the Valais Ocean.

## Acknowledgements

Martina Tribus is thanked for her help with electron probe microanalysis and Julia Wallraf for making the thin sections. We are very grateful to Chiara Groppo (Torino) and Paola Manzotti (Stockholm) for their constructive comments and suggestions that considerably helped to improve the manuscript.

## References

Anovitz L.M., Essene E.J., 1987. Phase equilibria in the system $CaCO_3$-$MgCO_3$-$FeCO_3$. Journal of Petrology, 28, 389–415. https://doi.org/10.1093/petrology/28.2.389

Ausich W.I., 1997. Regional encrinites: a vanished lithofacies: in Brett C.E., and Baird G.C., eds., Paleontological Events, Stratigraphic, Ecological, and Evolutionary Implications: Columbia University Press, New York, 509–519.

Barriga F.J.A.S., Fyfe W.S., 1983. Development of rodingite in basaltic rocks in serpentinites, East Liguria, Italy. Contributions to Mineralogy and Petrology, 84, 146–151. https://doi.org/10.1007/BF00371281

Bernoulli D., Jenkyns H.C., 1970. A Jurassic Basin: The Glasenbach Gorge, Salzburg, Austria. Verhandlungen der Geologischen Bundesanstalt, 4, 504–531.

Bertle R.J., 2002. Kreide und Paläogen in der Fimber-Zone (Unterengadiner Fenster, Schweiz–Österreich). Neue Mikrofossilfunde und deren paläogeographische Bedeutung. Eclogae Geologicae Helvetiae, 95, 153–167.

Bertle R.J., Frank W., Seward D., Jelenc M., Thöni M., Koller F., 2003. New Age Constraints on Alpine Metamorphism of the Schistes Lustrés of the Engadine Window based on Ar-Ar, Rb-Sr and Fission Track Dating. EGS-AGU-EUG Joint Assembly, Abstracts from the meeting held in Nice, France, 6–11 April 2003, abstract 14178.

Böhm F., 1986. Der Grimming: Geschichte einer Karbonatplattform von der Obertrias bis zum Dogger (Nördliche Kalkalpen, Steiermark). Facies, 15, 195–231. https://doi.org/10.1007/BF02536720

Bousquet R., Bertle R., Goffe B, Koller F., Oberhauser R., 2004. Day 4: HP/LT metamorphism within the North Penninic Ocean (Lower Engadine Window, Austria - Switzerland). In: Gosso G., Engi M., Koller F., Lardeaux J.M., Oberhänsli R., Spalla M.I. (eds.), Thermomechanical evolution of the Alpine Belt, from the Engadine Window to the Matterhorn, 32nd IGC Florence, Field Trip Guidebook B29, 22–27.

Bousquet R., Goffe B., Vidal, O., Oberhänsli R., Patriat M., 2002. The tectono-metamorphic history of the Valaisan domain from the Western to the Central Alps: new constraints on the evolution of the Alps. Geological Society of America Bulletin, 114, 207–225. https://doi.org/10.1130/0016-7606(2002)114%3C0207:TTMHOT%3E2.0.CO;2

Bousquet R., Oberhänsli R., Goffe B., Jolivet L., Vidal O., 1998. High-pressure – low-temperature metamorphism and Formation in the Bündnerschiefer of the Engadine window: implications for the regional evolution of the Central Alps. Journal of Metamorphic Geology, 16, 657–674. https://doi.org/10.1111/j.1525–1314.1998.00161.x

Cadisch J., 1932. Die Schichtreihe von Ardez (Steinsberg) im Unterengadiner Fenster. Eclogae Geologicae Helvetiae, 25, 17–22.

Corno A., Groppo C., Borghi A., Mosca P., Gattiglio M., 2023. To be or not to be Alpine: New petrological constraints on the metamorphism of the Chenaillet Ophiolite (Western Alps). Journal of Metamorphic Geology, 41, 745–765. https://doi.org/10.1111/jmg.12716

Daurer A., 1980. Short notes on the Idalp ophiolites (Engadine Window, Tyrol, Austria). Ofioliti, 5, 101–106.

De Capitani C., Petrakakis K., 2010. The computation of equilibrium assemblage diagrams with Theriak/Domino software. American Mineralogist, 95, 1006–1016. https://doi.org/10.2138/am.2010.3354

Dunham R.J., 1962. Classification of Carbonate Rocks According to Depositional Texture. American Association of Petroleum Geologists, Memoir, 1, 108–121.

Embry A.F., Klovan J.E., 1971. A Late Devonian reef tract on northeastern Banks Island, N.W.T.: Bulletin of Canadian Petroleum Geology v. 19, 730–781.

Fabricius F., 1967. Die Rät-und Lias-Oolithe der nordwestlichen Kalkalpen. Geologische Rundschau, 56, 140–170.

Fuchs G., Oberhauser R., 1990. Blatt 170 Galtür. Geologische Bundesanstalt, Vienna, Austria.

Gruber A., Pestal G., Nowotny A., Schuster R., 2010. Erläuterungen zu Blatt 144 Landeck, Geologische Bundesanstalt Wien, 200 pp.

Gruner U., 1981. Die jurassischen Breccien der Falknis–Decke und altersäquivalente Einheiten in Graubünden. Beiträge zur Geologischen Karte der Schweiz, Neue Folge, 154, 136 pp.

Gürler B, Schmutz H.U., 1995. Geologische Untersuchungen im SW-

Teil des Unterengadiner Fensters. Teil I, Geologie der Val Tasna und Umgebung. Beiträge zur Geologischen Karte der Schweiz, Neue Folge, 166, 123 pp.

Handy M.R., Schmid S.M., Bousquet R., Kissling E., Bernoulli D., 2010. Reconciling plate-tectonic reconstructions of Alpine Tethys with the geological-geophysical record of spreading and subduction in the Alps. Earth-Science Reviews 102, 121–158. https://doi.org/10.1016/j.earscirev.2010.06.002

Höck V., Koller F., 1989. Magmatic evolution of the Mesozoic ophiolites in Austria. Chemical Geology, 77, 209–227. https://doi.org/10.1016/0009-2541(89)90075-2

Höck V., Koller F., 1987. The Idalp ophiolite (Lower Engadine Window, Eastern Alps), its petrology and geochemistry. Ofioliti, 12, 179–192.

Höck V., Koller F., Oberhauser R., Ucik F., 1986. Exkursion E 1–4. Das Unterengadiner Fenster und sein Rahmen im Bereich Fimbertal-Samnaun verbunden mit einer Gesamtübersicht über den östlichen Fensterteil. Exkursionsführer zur Wandertagung 1986 der Österreichischen Geologischen Gesellschaft in Dornbirn, 107–122.

Höck V., Koller F., Bertle R., Bousquet R., 2004. Fimber unit and the Idalp ophiolite (South Penninic unit, Lower Engadine Window; Austria-Switzerland). In: Gosso G., Engi M., Koller F., Lardeaux J.M., Oberhänsli R., Spalkl M.I. (eds.), Thermo-Mechanical Evolution of the Alpine Belt, from the Engadine Window to the Matterhorn, 32. IGC Florence 2004, Field Trip Guidebook, B29, 19–22.

Holland T.J.B., Powell R., 1998. An internally consistent thermodynamic data set for phases of petrological interest. Journal of Metamorphic Geology, 16, 309–343. https://doi.org/10.1111/j.1525-1314.1998.00140.x

Holland T.J.B., Powell R., 2011. An improved and extended internally consistent thermodynamic dataset for phases of petrological interest, involving a new equation of state for solids. Journal of Metamorphic Geology, 29, 333–383. https://doi.org/10.1111/j.1525-1314.2010.00923.x

Hunziker J.C., Desmons J., Hurford A.J., 1992. Thity-two years of geochronological work in the Central and Western Alps: a review on seven maps. Mémoires de Géologie (Lausanne), No. 13, 59pp.

Koller F., 1985. Petrologie und Geochemie des Penninikums am Alpenostrand. Jahrbuch der Geologischen Bundesanstalt, Wien, 128, 83–150.

Koller F., Höck V., 1987. Die mesozoischen Ophiolithe der Ostalpen. Mitteilungen der Österreichischen Mineralogischen Gesellschaft., 132, 61–77.

Koller F., Höck V., 1990. Mesozoic ophiolites in the Eastern Alps. In: Malpas, J., Moores, E.M., Panayiotou, A., Xenophonthos, C. (eds.), Ophiolites – Oceanic Crustal Analogues, Nicosia, 253–263.

Koller F., Dlingeldey C., Höck V., 1996. Exkursion F: Hochdruck-Metamorphose im Recknerkomplex/Tarntaler Berge (Unterostalpin) und Idalp- Ophiolith/Unterengadiner Fenster. Mitteilungen der Österreichischen Mineralogischen Gesellschaft, 141, 305–330.

Krainer K., Mostler H., Haditsch J.G., 1994. Jurassische Beckenbildung in den Nördlichen Kalkalpen bei Lofer (Salzburg) unter besonderer Berücksichtigung der Manganerz-Genese. Abhandlungen der Geologischen Bundesanstalt 50, 257–293.

Leimser W., Purtscheller F., 1980. Beiträge zur Metamorphose von Metavulkaniten im Pennin des Engadiner Fensters. Mitteilungen der Österreichischen Mineralogischen Gesellschaft, 71/72, 129–137.

MacEachern J.A., Pemberton S.G., Gingras M.K., Bann K.L., 2010. Ichnology and facies models. In: James N.P., Dalrymple R.W. (eds.), Facies Models 4, Geological Association of Canada, GEOtext 6, 19–58.

Miller M.F., 1991. Morphology and paleoenvironmental distribution of Paleozoic *Spirophyton* and *Zoophycos*: Implications for the *Zoophycos* ichnofacies: Palaios, 6, 410–425. https://doi.org/10.2307/3514966

Mostler H., Krainer K., 1993. Neue Ophiuren aus liassischen Slope-Sedimenten der Nördlichen Kalkalpen in der Umgebung von Lofer (Salzburg). Geologisch-Paläontologische Mitteilungen Innsbruck, 19, 29–47.

Oberhauser R., 1976. Bericht 1975 über paläontologisch-sedimentologische Aufnahmen im Engadiner Fenster (Fimbertal) auf Blatt 170, Galtür. Jahrbuch der Geologischen Bundesanstalt, 158–159.

Oberhauser R., 1977. Bericht 1976 über paläontologisch–geologische Aufnahmen im Engadiner Fenster (Fimbertal) auf Blatt 170 (Galtür) und Blatt 171 (Nauders). Jahrbuch der Geologischen Bundesanstalt. 144.

Oberhauser R., 1980. Das Unterengadiner Fenster. In: Oberhauser R. (Hrsg.): Der Geologische Aufbau Österreichs, Springer Verlag, Wien, 291–297.

Oberhauser R., 1984. Bericht 1983 über geologische Aufnahmen im Unterengadiner Fenster auf Blatt 170 Galtür. Jahrbuch der Geologischen Bundesanstalt, pp. 250–251.

Oberhauser R., 2007. Profilschnitt vom Bodensee ins Unterengadin. Beilage in: Oberhauser R., Bertle H., Bertle R. (eds.), Geologische Karte von Vorarlberg 1:100 000. Geologische Bundesanstalt, Wien.

Pettijohn F.J., Potter P.E., Siever R., 1987. Sand and Sandstone: Springer-Verlag (2nd edition), New York, 553.

Powell R., Holland T.J.B., 2006. Course Notes for 'THERMOCALC Short Course'. Sao Paulo, Brazil, on CD-ROM.

Schmid S.M., Fügenschuh B., Kissling E., Schuster R., 2004. Tectonic map and overall architecture of the Alpine orogen. Eclogae Geologicae Helvetiae, 97, 93–117. https://doi.org/10.1007/s00015-004-1113-x

Schmid S.M., Scharf A., Handy M.R., Rosenberg C.L., 2013. The Tauern Window (Eastern Alps, Austria): a new tectonic map, with cross-sections and a tectonometamorphic synthesis. Swiss Journal of Geosciences, 106, 1–32. https://doi.org/10.1007/s00015-013-0123-y

Schuster R., Koller F., Höck V., Hoinkes G., Bousquet R., 2004. Explanatory notes to the map: metamorphic structure of the Alps metamorphic evolution of the Alps. Mitteilungen der Österreichischen Mineralogischen Gesellschaft, 149, 63–87

Theobald G., 1864. Geologische Beschreibung der nordöstlichen Gebirge von Graubünden. Beiträge zur geologischen Karte der Schweiz 2.

Thum I., 1966. Zur Geologie des Unterengadiner Fensters (im Raum Spiß – Nauders, Oberinntal). Unpublished Ph.D. thesis, University of Vienna, 169 pp.

Thum I., 1970. Neuere Daten zur Geologie des Unterengadiner Fensters (unter besonderer Berücksichtigung der Schwermineralanalysen). Mitteilungen der Österreichischen Geologischen Gesellschaft, 62, 55–77.

Tollmann A., 1976. Analyse des Klassischen Nordalpinen Mesozoikums. Franz Deuticke, Wien, 576 pp.

Tollmann A., 1977. Geologie von Österreich. Band I. Die Zentralalpen. Franz Deuticke, Wien, 766 pp.

Tropper P., Krainer K., 2017. Walking on Jurassic Ocean Floor at the Idalpe (Engadine Window) near Ischgl, Tyrol. Mitteilungen der Österreichischen Mineralogischen Gesellschaft, 163, 117–128.

Waibel A.F., Frisch W., 1989. The Lower Engadine Window. Sediment deposition and accretion in relation to the plate-tectonic evolution of the Eastern Alps. Tectonophysics, 162, 229–241. https://doi.org/10.1016/0040-1951(89)90246-1

Wiederkehr M., Sudo M., Bousquet R., Berger A., Schmid S.M., 2009. Alpine orogenic evolution from subduction to collisional thermal overprint: The $^{40}Ar/^{39}Ar$ age constraints from the Valaisan Ocean, central Alps. Tectonics, 28, 1–28. https://doi.org/10.1029/2009TC002496

Zhang L.J., Fan RY., Gong Y.M., 2015. Zoophycos macroevolution since 541 Ma. Scientific Reports 5, 14954. https://doi.org/10.1038/srep14954

Zimmermann R., Hammerschmidt K., Franz G., 1994. Eocene high-pressure metamorphism in the Penninic units of the Tauern Window (Eastern Alps): Evidence from $^{40}Ar–^{39}Ar$ dating and petrological investigations. Contributions to Mineralogy and Petrology, 117, 175–186. https://doi.org/10.1007/BF00286841

Received: 8.10.2024
Accepted: 23.1.2025
Editorial Handling: Kurt Stüwe